universität wien

DIPLOMARBEIT

Titel der Diplomarbeit

B-Raf in tumor-driven angiogenesis

Verfasserin

Barbara Maier

angestrebter akademischer Grad

Magistra der Naturwissenschaften (Mag.rer.nat.)

Wien, 2011

Studienkennzahl lt. Studienblatt:	A 490
Studienrichtung lt. Studienblatt:	Diplomstudium Molekulare Biologie
Betreuerin / Betreuer:	Prof. Dr. Manuela Baccarini

Table of contents

1. Abstract

Tumor blood vessels display characteristics that distinguish them from vessels in healthy tissues. They form a hyperdense meshwork and are in general less functional than normal blood vessels. This is due to decreased pericyte coverage, unstable perfusion and increased vascular permeability. All these features lead on the one hand to insufficient nutrient and oxygen delivery and on the other hand impede the uniform targeting of the tumor with drugs.

We show that B-Raf, the main activator of Erk in the MAP kinase signaling cascade, contributes to hyperpermeability of blood vessels in a tumor environment. We analyzed a mouse with conditional knock-out of B-Raf in endothelial cells and hematopoietic cells, B-Raf EC KO. Those mice show accelerated tumor growth of LLC-1 allografts. The tumors show decreased necrotic areas, however, the number of blood vessels within the tumor stays unchanged. We hypothesize, that the functionality of tumor vessels in B-Raf EC KO mice is restored and that the vasculature is normalized compared to control, which could lead to the observed accelerated tumor growth.

We find that perfusion of vessels is not affected in B-Raf EC KO mice. In addition pericyte coverage is unchanged compared to control. With the so-called Miles Assay, an in vivo-assay that determines permeability of skin blood vessels, we could demonstrate that the B-Raf EC KO mice are more resistant to VEGF induced permeablity compared to control mice shown by a reduced extravasation of Evans Blue. Furthermore we show that B-Raf EC KO mice have a lower basal level of vessel permeability in the LLC-1 tumor compared to control mice. In vitro we determine the barrier function of the endothelial cells by performing an impedance measurement of an endothelial cell monolayer. We find that B-Raf KO endothelial cells show a lower permeability specifically after VEGF stimulation than control cells. To rule out a possible role for the myeloid lineage, which is deleted for B-Raf in the B-Raf EC KO mice, we analyzed the growth of LLC-1 allografts in mice lacking B-Raf specifically in the myeloid compartment. In this mice tumor growth is unchanged.

Our results indicate a role for endothelial B-Raf in contributing to a state of hyperpermeability in tumor blood vessels. This could be of special relevance in tumor therapy, where specific inhibitors for B-Raf are currently in clinical trials.

1. Zusammenfassung

Tumorblutgefäße zeichnen sich durch einige Eigenschaften aus, die sie von Gefäßen in anderen Geweben unterscheiden. Sie formen ein übermäßig dichtes Netzwerk, sind aber generell weniger funktionell als normale Blutgefäße. Das resultiert aus geringer Perizytenanlagerung, unregelmäßiger Durchblutung und hoher Permeabilität. Diese Charakteristika sind zum einen für den ungenügenden Transport von Nährstoffen und Sauerstoff verantwortlich, zum anderen erschweren sie es, den Tumor gleichförmig medikamentös zu behandeln.

Wir können nun zeigen, dass B-Raf, der Hauptaktivator von Erk im MAP Kinase Signaltransduktionsweg, zur Hyperpermeabilität von Blutgefäßen in einem Tumorumfeld beiträgt. Wir haben einen Mausstamm mit einem konditionellen Knock-out von B-Raf in Endothelzellen untersucht; B-Raf EC KO. Diese Mäuse zeigen beschleunigtes Tumorwachstum von injizierten LLC-1 Allografts. In den Tumoren wurden weniger nekrotische Bereiche gefunden, die Anzahl an Blutgefäßen ist aber gleich. Wir haben die Hypothese aufgestellt, dass die Funktionalität von Tumorblutgefäßen wieder hergestellt ist und das Gefäßsystem normalisiert ist im Vergleich zur Kontrolle. Diese Annahme stützt auch das beschleunigte Tumorwachstum, das wir in den Mäusen beobachten.

Wir konnten zeigen, dass die Durchblutung der Gefäße in B-Raf EC KO Mäusen nicht betroffen ist. Perizytenanlagerung war ebenfalls nicht verändert im Vergleich zur Kontrolle. Mit dem so genannten Miles-Assay, ein in vivo Test, der die Permeabilität von Blutgefäßen der Haut bestimmt, konnten wir zeigen, dass B-Raf EC KO Mäuse Defekte in der Regulierung ihrer sogenannten Barriere-Funktion nach Stimulation mit VEGF haben. Außerdem haben B-Raf EC KO Mäuse ein geringeres basales Permeabilitätslevel ihrer Tumorgefäße. In vitro führten wir eine Impedanzmessung durch, die Informationen über die Barriere-Funktion der Zellen gibt. Das Ergebnis ist, dass B-Raf KO Endothelzellen ihre Permeabilität nach einem VEGF Stimulus nicht hinauf regulieren können. Die Zellen haben also den selben Defekt, den wir auch in vivo durch den Miles Assay zeigen konnten.

Um eine mögliche Beteiligung der myeloiden Zelllinie, die in B-Raf EC KO Mäusen ebenfalls für B-Raf deletiert ist, auszuschließen, haben wir das Wachstum von LLC-1 Allografts in Mäusen defizient für B-Raf spezifisch im myeloiden Kompartment analysiert. In diesen Mäusen ist das Wachstum von LLC-1 Tumoren nicht verändert.

Unsere Resultate weisen darauf hin, dass B-Raf in Endothelzellen zu einer erhöhten Permeabilität in Tumorblutgefäßen beiträgt. Dieses Ergebnis könnte von großer Relevanz in der Tumortherapie sein, wo spezifische B-Raf Inhibitoren bereits in klinischen Studien getestet werden.

2. Introduction

2.1. Architecture of blood vessels

In vertebrates, blood vessels form a tight meshwork of arteries, veins and capillaries through the whole organism, allowing all tissues and peripheric areas of the body to be perfused with blood and thereby supplied with oxygen and nutrients. Immune cells, but also cancer cells use blood vessels as highways on which they can move through the whole organism.

The supply of nutrients and oxygen as well as the clearance of CO_2 and metabolic waste products from the tissues occurs via microvascular capillaries, the most abundant type of vessel. They consist only of a tube of endothelial cells (ECs) surrounded by a basement membrane secreted by the endothelial cells themselves as well as from vessel specific supporting cells such as vascular smooth muscle cells (vSMCs) and pericytes. Pericytes that are embedded in the basement membrane stabilize the endothelial tube and keep it in a quiescent state. Capillaries have organ-specific characteristics such as fenestrations that occur in kidney and in endocrine glands. Arteries and veins are larger vessels that transport blood with high efficiency for long distances within the body. Arteries transport oxygenated blood from the heart into smaller arterioles and into the capillary bed of the body. Veins transport the deoxygenated blood from peripheric tissues back to the heart and finally to the lungs, where the blood is reoxygenated. Arteries and veins both consist of three different layers: The Intima, which is the endothelial cell tube with an internal elastic lamina; the Media, made out of smooth muscle cells that stabilize the EC tube surrounded by an external elastic lamina; and the Adventitia that consists of fibroblasts and extracellular matrix. In contrast to the loose pericyte coverage found in capillaries, the larger arteries and venes are highly covered with multiple layers of vascular smooth muscle cells. Arterioles and venules are vessels of medium size (Fig.1.) [1-2].

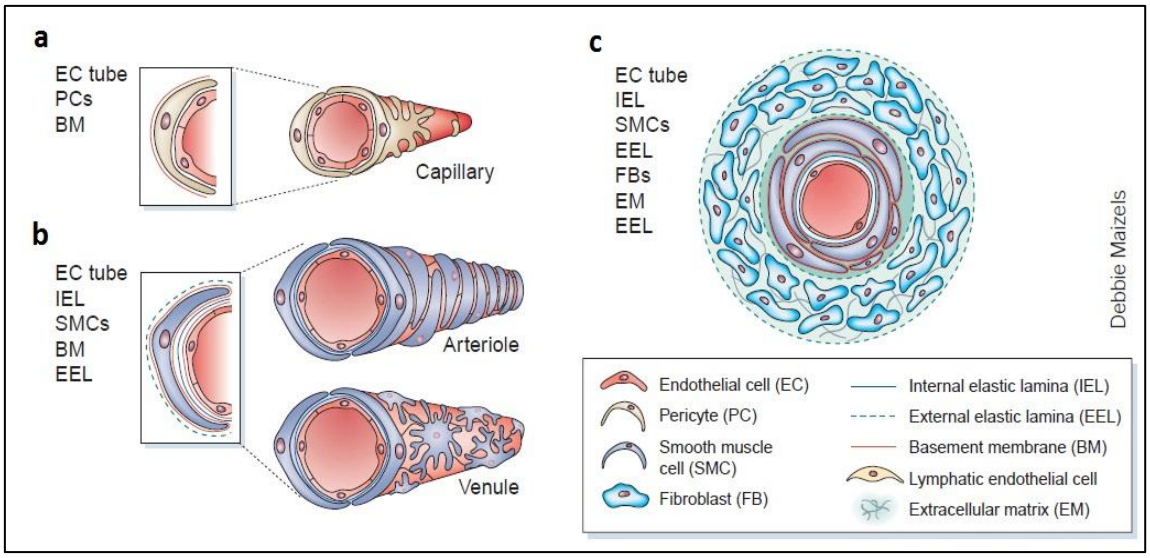

Fig.1. modified from [1]. Overview of different types of blood vessels.

2.2. The formation of blood vessels: vasculogenesis and angiogenesis

Angiogenesis and vasculogenesis are the two types of blood vessel growth. Vasculogenesis refers to primary formation of the blood system in the developing embryo, whereas angiogenesis is the growth of blood vessels from preexisting ones. The formation of blood vessels is under tight regulation. Angiogenic and vasculogenic growth requires precise coordination of cell proliferation, differentiation, migration, matrix remodeling and various signaling processes between different cell types. After embryonic development angiogenesis occurs in wound healing, growth of tissues (e.g. fat tissue), tissue remodeling (e.g. endometrium) and in a number of pathologies. Vasculogenesis is a completed process after embryogenesis.

In vasculogenesis the precursors of endothelial cells, the angioblasts, form the vascular plexus that subsequently develops into primitive blood vessels. The most prominent factor in vasculogenesis and angiogenesis is vascular endothelial growth factor (VEGF). VEGF is crucial for the generation of blood vessels, since mice heterozygous for VEGF-A or its receptor (Flk1, also called VEGFR2) die *in utero* because of the lack of blood vessels and hematopoietic cells[3-5]. Mice lacking VEGF receptor 1 (VEGFR1) are able to form angioblasts, but the assembly of vessels is impaired [6]. Newly developed

vessels become stabilized by the recruitment of mural cells and by the establishment of a basement membrane. VEGF signaling stimulates ECs to secrete platelet derived growth factor B (PDGF-B), which in turn stimulates migration and proliferation of pericytes [7]. Also other factors secreted by endothelial cells, such as S1P-1 and angiopoietins, are implicated in the attraction of pericytes [8]. Mural cells produce Ang1 and thereby stabilize vessels and prevent them from leaking. ECM formation is driven by TGF-ß1 which is secreted by ECs [1, 9].

Once the first blood vessels are formed, further growth of the vascular system occurs by angiogenesis. In angiogenesis, new vessels form from pre-existing ones through sprouting. Angiogenesis is initially stimulated by the secretion of VEGF, induced in turn by the oxygen sensor HIF-1 whenever low levels of oxygen are detected within the tissue [10]. Together with other pro-angiogenic factors such as FGF [11], Ang-2, and under certain conditions also Ang-1 [12], VEGF stimulates ECs that are incorporated in blood vessels to change their state from quiescent to active, rendering them able to proliferate and to migrate.. First, the ECM and basement membrane need to be remodeled locally to give the forming tip cell the opportunity to grow out of the preexisting vessel. The tip cell is the leading endothelial cell sprouting out of the vessel. It forms dynamic filopodia that scan the environment for further growth factors, and therefore guides the proliferating stalk cells, ECs forming the stem of the sprout, to sites were high levels of VEGFA are secreted [2]. To form a perfused vessel, the tip cell needs to contact another vessel or tip cell. At this point, strong cell-cell contacts are established, mural cells are recruited, ECM is deposited and a vessel lumen is generated.

2.3. The role of pericytes in the vascular system

In an adult organism, endothelial cells are usually in a quiescent state that is maintained by signaling from pericytes and vascular smooth muscle cells (vSMCs). Pericytes are attracted to developing blood vessels by PDGF-B secreted from ECs and

wrap around the endothelial cell tube, regulating different vessel parameters [14] (Fig.2). Pericytes can contract or relax depending on outside stimuli and therefore regulate vessel diameter and capillary blood flow [13]. In general, vessels that are under high blood pressure show more pericyte coverage [14]. Pericytes are also necessary to establish the blood-brain barrier, which indicates an essential role in vessel integrity. Besides providing mechanical stability to the vessel, the pericytes contribute to maintaining ECs in a non-proliferative and non-migratory state through direct signaling.

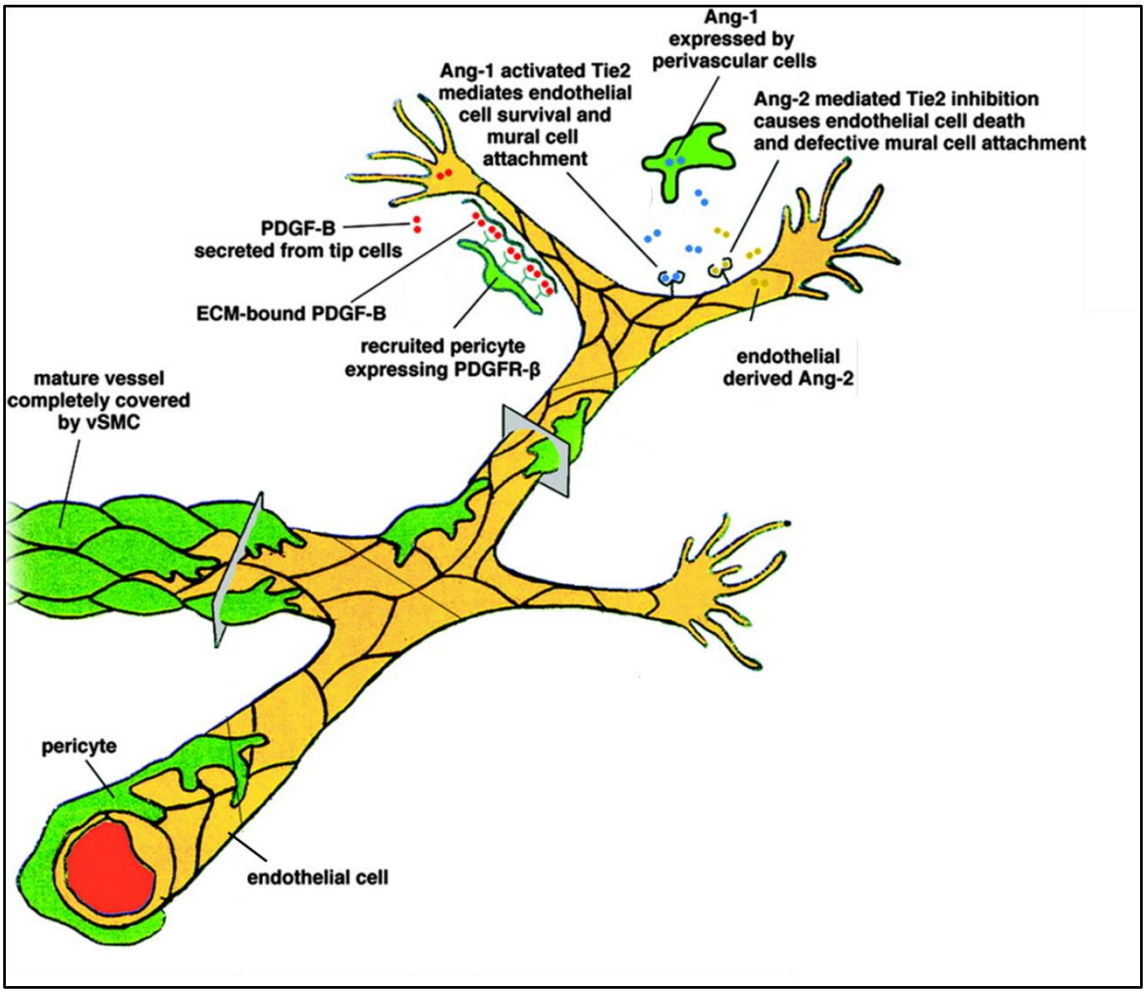

Fig.2. Modified from [15]. Signaling pathways in pericyte attraction and vessel stabilization

One important paracrine signaling pathway is that of angiopoietins and their receptors Tie. Ang-1 produced by pericytes maintain the quiescent state and promote survival of ECs, whereas Ang-2 derived from the ECs in contrast loosens the contact between ECs and pericytes and can eventually lead to an active, sprouting state of the endothelial cells in the presence of VEGF [13] (Fig2). Another signaling pathway that influences endothelial/pericyte interaction is the Sphingosine-1 phosphate (S1P) pathway. Produced by hematopoietic cells and platelets, S1P supports trafficking of the adhesion molecule N-Cadherin to adherens junctions in ECs, thereby stabilizing the contact between ECs and pericytes. The differentiation of pericytes is mainly achieved through TGF-β that is mobilized by the endothelial cells. Taken together, pericytes are important regulators of blood vessel maintenance and growth.

2.4. Characteristics of tumor blood vessels

In normal tissue, a very sensitive balance between pro- and anti-angiogenic factors ensures that blood vessels are correctly formed and matured and that angiogenesis occurs only in a controlled and restricted manner. Many diseases like obesity, rheumatoid arthritis, diabetic retinopathy and solid tumors require angiogenesis. Pathological angiogenesis is very disorganized and uncontrolled. This holds also true for blood vessel formation in solid tumors. A tumor larger in size than $2mm^3$ can no longer be provided with oxygen by diffusion, wherefore tumor blood vessels need to be formed [16]. Due to the imbalance of angiogenic factors produced during tumor-induced angiogenesis, vessels formed under pathological conditions are usually abnormal in their structure and function. Tumor blood vessels have various features that distinguish them from vessels in normal tissue. Many tumors produce large amounts of angiogenic stimulators, resulting in hyperactive vessel growth without stabilization of the newly formed vessels [8].Tumor vasculature is characterized by an abnormally high vessel density, because anti-angiogenic factors that restrict growth of sprouts are missing. Despite their number, however, these vessels are less functional

and don’t supply the tumor efficiently with oxygen and nutrients. The resulting hypoxia leads to a vicious circle of production of more angiogenic factors and, as a result, to even more anomalous vessels [17]. The architecture of tumor blood vessels is usually described as tortuous, disorganized and irregular. Because stabilizing factors are not present, tumor blood vessels may lack pericyte coverage and even a basement membrane. Interestingly, VEGF itself leads to impaired pericyte coverage of vessels. Mechanistically, VEGF binds to the VEGFR-2 expressed on the pericyte/vSMC and inhibits PDGFRβ signaling by forming a VEGFR-2/PDGFRβ heterodimer [18]. Endothelial cells can be very abnormal in the tumor with gaps in between cells, fenestrations and impaired signaling. Usually, tumor blood vessels are also hyperpermeable which leads to a very bad nutrient supply and high rates of necrosis in the inner part of the tumor. This is linked to the enhanced permeability and retention (EPR) effect, which describes the retention of molecules of more than 50kDa in size specifically in tumor tissue [19] – a phenomenon which based on the abnormally high permeability of tumor vessels (Fig.3.).

The vessels in a tumor display great heterogeneity. In some regions so-called blood lakes form, where big hollow spaces in the tumor are filled with blood. These “lakes” are not part of the circulation and don’t participate in nutrient supply. In addition, the direction of the blood flow may vary, since there is no clear distinction between arteries and veins in the tumor. All of these defects result in an acidic, hypoxic environment that favors

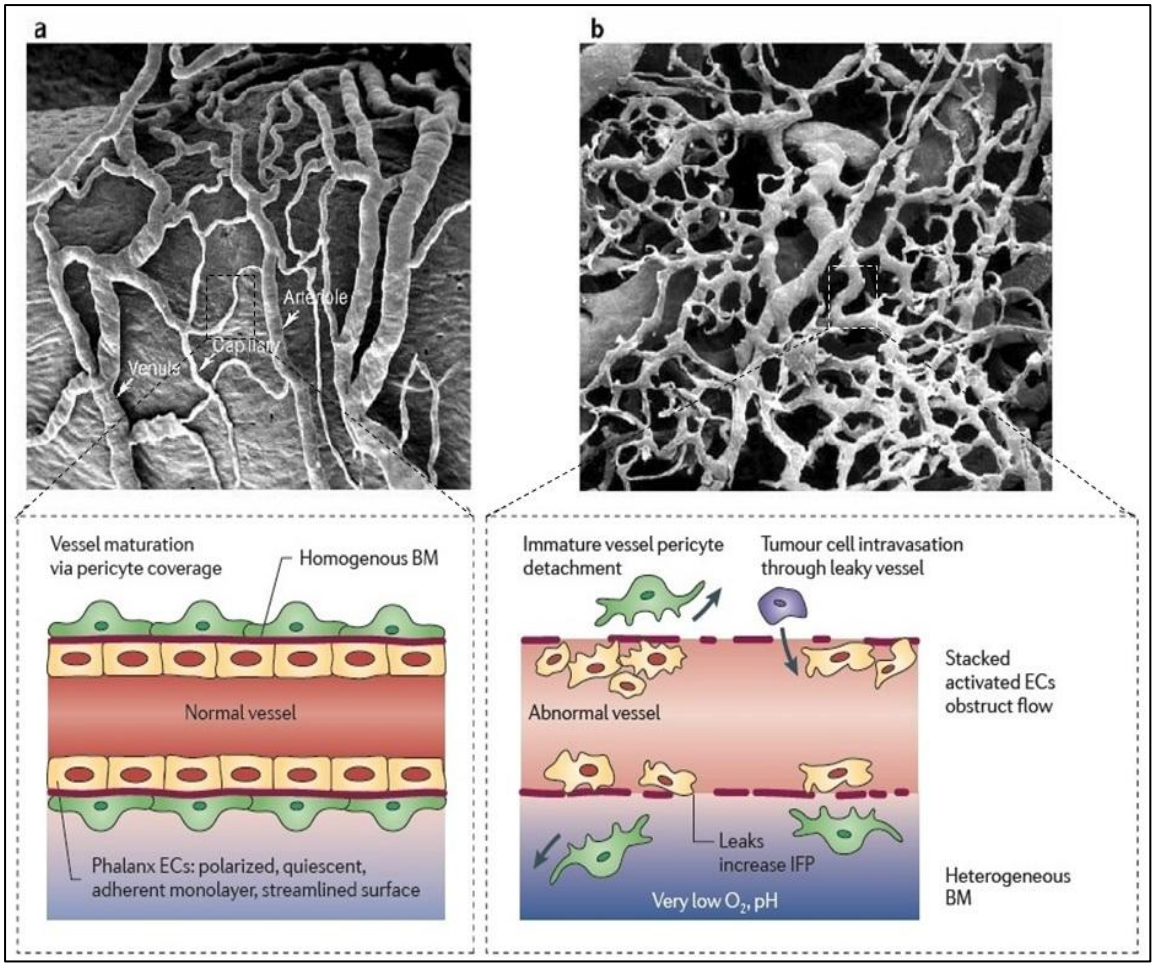

Fig.3. Modified from [20]and [21]. a. normal vs. b. tumor blood vessels.

malignancy and metastasis and negatively affects the delivery of chemotherapeutics [21-24].

2.5. Anti-angiogenic therapy

Since it became clear that all solid tumors, irrespective of their origin, need angiogenesis, tumor blood vessels have been a promising target for cancer treatment. The initial approach was to inhibit further vessel growth and/or destroy existing tumor vessels to starve the cancer cells and ideally lead to tumor shrinkage [25]. VEGF is the most important factor in promoting tumor angiogenesis and it is overexpressed at high frequency in many cancers. Therefore, anti-VEGF therapy is the most tested anti-angiogenesis therapy, although other potential targets have been investigated. A

monoclonal antibody against VEGF is now approved for the treatment of several types of cancer. So far, anti-angiogenic treatment has achieved only moderate success. In patients, it delays tumor progression for a few months at best [26-27]. The reason for this rather disappointing results is that tumors can adapt rapidly to anti-angiogenic therapy and evolve strategies for resistance, for example by upregulation of alternative pro-angiogenic signaling pathways, recruitment of bone-marrow derived cells that stimulate angiogenesis, enhanced pericyte coverage, and metastasis [28]. This means that anti-VEGF therapy can even drive tumor progression. On the other hand, it has also been shown that anti-angiogenic therapy can be quite successful in the combination with chemotherapy.

Many abnormalities of the tumor vasculature are direct or indirect effects of the high level of VEGF signaling in the tumor. Therefore it has been hypothesized that anti-VEGF therapy might also lead to a normalization of tumor vessels [23]. This normalization ideally would lead to more functional and less leaky vessels able to transport blood into all parts of the tumor equally well. As a consequence, primary tumor growth would not be restricted, but the efficacy of chemotherapy could be enhanced because of increased delivery of chemotherapeutic agents. These drugs could then act on all parts of the tumor and therefore lead to uniform shrinkage [26-27].

In conclusion, anti-VEGF therapy can have different effects on tumor growth depending on the origin, on the genetic setup and on the VEGF-dependence of a tumor.

2.6. Vascular permeability

2.6.1 Transcellular and Paracellular molecular transport

The most fundamental functions of blood circulation - distributing oxygen and nutrients in the organism and giving immune cells a highway which they can enter and leave at distant body sites - are highly linked with vessel permeability. Endothelial

transport can occur in a transcellular or paracellular way. Solutes with a radius up to 3nm can move passively through the endothelial barrier by the paracellular route, i.e. just by diffusing between 2 endothelial cells. Active transport of macromolecules occurs via the transcellular route, which means crossing an endothelial cell in a vesicle [29] (Fig.4.). Transcytosis occurs following the interaction of plasma proteins with specific docking molecules on caveolae on the surface of endothelial cells [30].Transcellular transport is regulated by cellular adhesive forces, whereas paracellular transport is regulated by modifying interendothelial junctions (IEJs). Inflammatory effectors like Thrombin, VEGF, bradykinin, histamine and others modify permeability via disrupting the organization of IEJs and integrin-ECM complexes. This opens intercellular gaps and allows passage of proteins [31]. The composition of the extracellular matrix (ECM) and of the basement membrane has also an impact on vessel permeability, as well as the interactions between ECs and ECM influence overall permeability. Vessels from different organs and different size have of course individual differences in those parameters and in permeability.

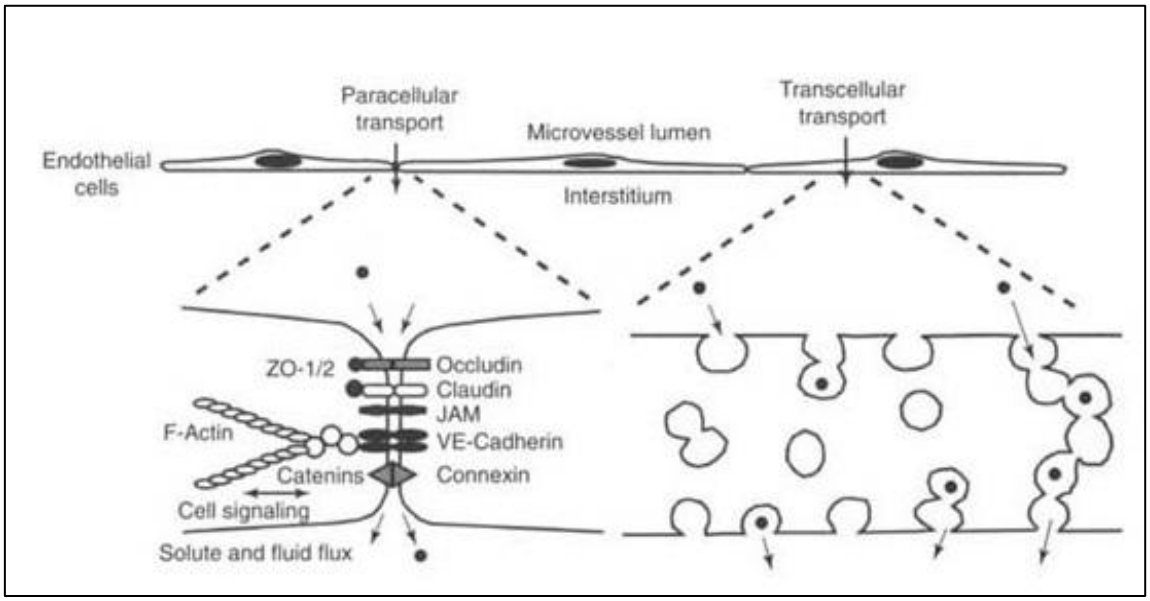

Fig.4. [32]. Paracellular transport (left) vs. transcellular transport (right).

2.6.2 The role of Adherens junctions in vascular permeability

Adherens Junctions, which are mediated by the homophilic interaction among VE-Cadherin (VEC) molecules on different endothelial cells are necessary for establishment of a barrier function.. Deletion of VEC in mice leads to lethality due to an immature vasculature. Tight Junctions and Gap Junctions are also necessary for the endothelial barrier formation, although their role is less studied so far [33].

Various signaling pathways regulate endothelial permeability. Most of them stimulate the formation or disruption of IEJs. Various modifications of VEC that have been discovered influence vascular permeability. For example, phosphorylation of certain residues in VEC or one of its adaptor proteins, β-catenin, modulate the strength of adherens junctions. Furthermore, internalization of VEC after VEGF stimulation, or cleavage of VEC by different metalloproteases (MMPs) has been shown to lower the endothelial barrier function. Conversely, high cellular levels of cyclic adenosin monophosphate (cAMP) promote barrier function by strengthening VEC structures.

2.6.3 Factors modifying vascular permability

VEGF, which was also identified as vascular permeability factor (VPF), is known to stimulate vascular permeability via its receptor Flk-1 [34]. Flk-1 activates many signaling pathways, amongst them Ras, PI3K, PKC and PLC [35]. It is yet unclear which of these pathways is involved in regulating vascular permeability. Conflicting results have been reported, for instance, on the role of MEK : Wu et al. showed that VEGF induced permeability of rat venules is blocked by MEK inhibition [36]. In contrast, in frog microvessels MEK inhibition had no effect [37]. However, it is known that VEGF stimulates vascular permeability via elevating intracellular Ca^{2+} levels which in turn leads to the internalization of VEC [38].As a consequence, cell-cell contacts loosenand paracellular permeability increases.[38] . Additionally, VEGF induced elevated Ca^{2+}

levels lead to increased vesicle fusion and therefore increased transcellular permeability [33].

Other permeability stimulating factors, such as the bacterial endotoxin LPS, the coagulation factor Thrombin and the cytokine TNF-α, induce vascular permeability also by elevating Ca^{2+} levels, although the second messengers vary between the different signaling pathways and are not yet fully understood. Factors opposing permeability are S1P and Ang-1, which lead to assembly of AJs and thereby strengthening of barrier function. [33]. .

2.7. Tumor associated macrophages - TAMs

Immune cells are reported to have different roles in tumorigenesis. For macrophages it is known that the different subclasses M1 and M2 have opposing effects. Classically activated M1 macrophages respond to stimuli like LPS or IFN-γ. They produce pro-inflammatory cytokines and kill microorganisms and tumor cells and are therefore tumor repressing [39].The alternatively activated population of M2 macrophages responds to anti-inflammatory chemokines such as IL-4 and IL-10. M2 macrophages participate in anti-inflammatory processes, Th1 immunity, tissue repair and angiogenesis and are therefore considered tumor-promoting [39-40]. Tumors actively recruit macrophages by secreting macrophage colony stimulating factor (M-CSF) and other attracting chemokines [41]. Tumor associated macrophages (TAMs) can have an M1 or M2 phenotype, depending on the signaling factors present in the tumor [42]. Usually, a high number of TAMs correlates with bad prognosis, which indicates that the majority of macrophages might be the tumor promoting M2 type in many tumors. Macrophages may promote tumorigenesis in different ways, for example by secreting matrix metalloproteases (MMPs) which enhance tumor invasiveness [43], growth factors stimulating tumor cell growth , and/or pro-angiogenic factors such as VEGF and FGF which promote angiogenesis [41].

A subpopulation of monocytes Tie2 expressing monocytes (TEMs), has very high pro-angiogenic potential. TEMs are attracted by tumor or Tumor-associated endothelial cells secreting Ang-2, [44], and enhance tumor angiogenesis by secreting angiogenic factors and MMP9, which leads to the release of growth factors from ECM [45-46].

2.8. MAP kinase pathway

The MAP kinase pathway is one of the major signaling pathways regulating cell proliferation, differentiation and apoptosis. The best-known mitogen-activated protein kinase pathway is the Ras – Raf – Mek – Erk pathway, activated by many extracellular stimuli including the binding of growth factors to receptor tyrosine kinases. Once the receptor is activated, the nucleotide exchange factor SOS is recruited to the plasma membrane and activates the small G-protein Ras. As a consequence, GDP is released from Ras, allowing the binding of GTP. GTP-loaded Ras can bind and thereby activate the serine/threonine kinase Raf. Subsequently, Raf activates its substrate MEK, which in turn phosphorylates and thereby activates ERK. Once ERK is activated, it can modify numerous target proteins in the nucleus as well as in the cytosol, thereby affecting cell motility, metabolism, differentiation, proliferation, survival or apoptosis. Since the outcome of Erk signaling changes very fundamental features of a cell, many levels of pathway modulation exist. Scaffolding platforms or proteins that bind and/or manipulate one of the pathway steps or ERK substrates can modify and fine-tune the outcome of Ras-Raf-MEK-ERK cascade signaling. Therefore the result of MAP kinase pathway activation can vary strongly between cell types and cell cycle stages and the organization of MAP kinase signaling *in vivo* takes place in an extremely complex manner (Fig.5.).

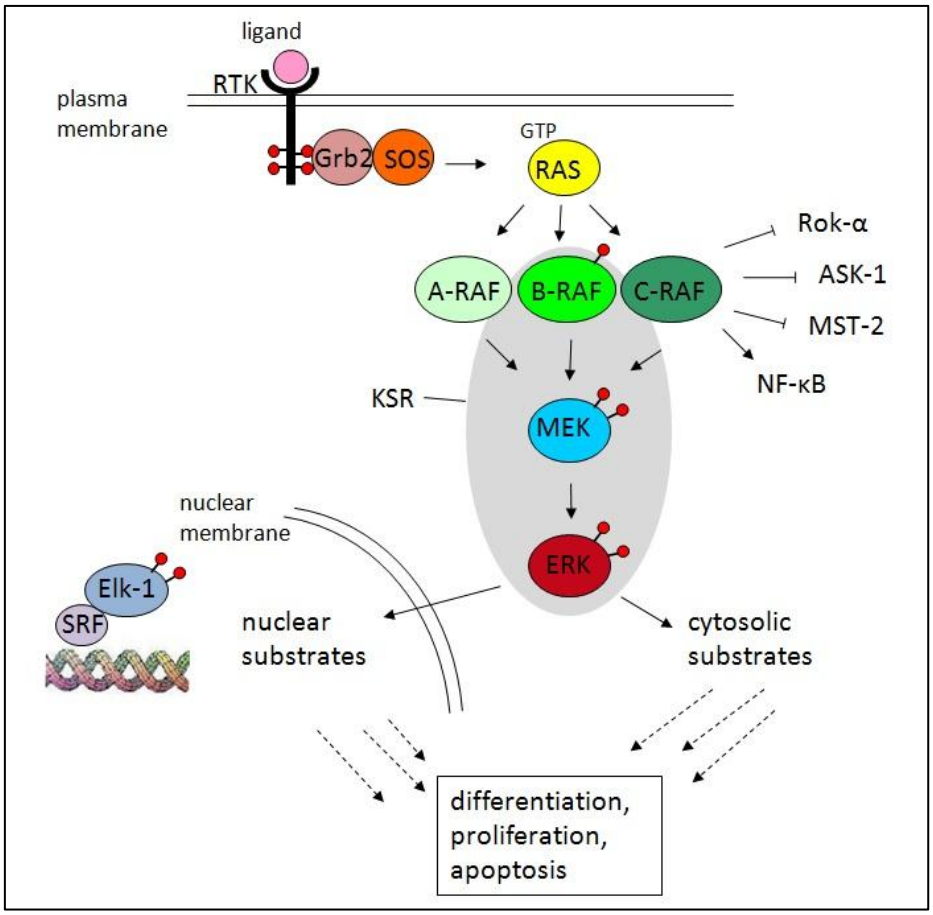

Fig.5. Simplified overview of the Ras signaling pathway.

Mammals express 3 different isoforms of Raf, namely A-Raf, B-Raf and C-Raf [47]. All 3 forms of Raf have 3 highly conserved domains, the carboxyterminal kinase domain and 2 N-terminal regulatory domains, which are necessary for the binding to Ras and to several other proteins. Ablation of A-Raf in mice does not yield a developmental phenotype, but leads to neuronal defects in the adult mouse [48]. The individual function of A-Raf is not known so far, but B-Raf and C-Raf seem to be more crucial for Erk activation. Whereas B-Raf is not known to interfere with other signaling pathways, C-Raf can bind to and thereby inhibit Ask-1, MST-2 and Rok-αand activate NF-κB.. C-Raf ablation is embryonic lethal because of apoptosis of embryonic liver cells [49-51]. Knock-out of B-Raf is also embryonic lethal, due to vascular defects of the placenta [52-53]. B-Raf KO embryos supported by a wildtype placenta are born at term but die from severe neurodegenerative disease around postnatal day 21 [53].

2.9. The Ras pathway in cancer

The activity of the Ras-Raf pathway is frequently altered in human and murinecancers. In particular, activating point mutations of Ras are found frequently in pancreatic cancer (58%), lung cancer (17%) and colon cancer (33%). In addition, activating mutations in B-Raf are frequent events in a subset of malignancies, such as melanoma (43%), thyroid cancer (39%) and colon cancer (12%) [54], although studies on mutation frequencies in human cancer must be treated with caution, since they are limited by sample numbers and by the possible statistically not representable choice of patients. The most frequent mutation is B-Raf V600E, which leads to a constitutively active B-Raf kinase with about 700-fold increase of kinase activity compared to wildtype [55]. On the contrary, mutations in C-Raf and A-Raf are extremely rare.

Because of the high frequency of activating mutations, the pathway is a promising target for cancer therapy. Strategies to inhibit Ras and MEK have been designed. but have failed; in the case of Ras, inhibition of farnesylation, which is required for Ras activation, has been attempted but failed because this modification can be carried out by a number of redundant regulators. MEK inhibitors, on the other hand, have marked side effects, and therefore a reduced therapeutic window. Raf inhibition by Sorafenib is quite successful in the treatment of renal-cell carcinoma, most likely because of its anti-angiogenic properties. Second generation, more specific inhibitors of B-Raf are currently in clinical trials. PLX4032/RG7204 and GSK2118436 have showed a high response rate in patients, although in some patients new cancers arose. This paradox might be due to a transactivation of Raf dimers in cells that are wildtype for B-Raf [56].

Overall, the fact that the Ras-Raf pathway is a prime target of molecule-based strategies for cancer treatment stresses the need of obtaining more knowledge about the essential functions of its component.

2.10. Knock-out of B-Raf in endothelial cells: B-Raf Tie2Cre mice

Because B-Raf knock-out animals die from defects of the vasculature in the placenta, it is likely that B-Raf has a key function in endothelial cells [52-53]. To test this hypothesis, a mouse line, carrying two floxed alleles of B-Raf (exon 12 of the B-Raf gene is flanked by loxP sites) and expressing the Cre recombinase under the control of a Tie2 promotor (Tie2Cre) has been generated. Tie2 is expressed in endothelial as well as in hematopoietic cells, including macrophages, granulocytes, dendritic cells, B-cells, T-cells and NK cells [44, 57]. Deletion of B-Raf in B-Raf Tie2Cre mice was assessed by PCR and Western Blot. In endothelial cells the deletion of B-Raf is very efficient, whereas in bone marrow deletion efficiency varies. However, bone marrow cells stimulated with Lewis lung carcinoma (LLC-1) cell conditioned medium show increased expression of the Tie2 receptor, accompanied by more efficient deletion. This suggests that within the tumor environment, recombination of the floxed allele in bone marrow derived cells can be very efficient. Spleen lysates did not show significant deletion of B-Raf, which indicates that B-cells and T-cells are not efficiently deleted. [Scherrer K., unpublished data or [58]]

B-Raf Tie2Cre mice do not show any gross defects in development or later in life, suggesting that B-Raf is not essential for tissue or vessel homeostasis.. Tissue architecture is normal and the number of blood vessels in different tissues is also unaffected. To monitor pathologic neo-vascularization, LLC-1 cells were injected subcutaneously and tumor growth in B-Raf Tie2Cre mice was measured. Surprisingly, endothelial B-Raf ablation accelerated tumor growth. Proliferation and apoptosis were unchanged but necrosis was significantly reduced at later stages of tumor progression in the tumors growing in the B-Raf deficient animals [Scherrer K., unpublished data].

Endothelial B-Raf ablation did not affect the density of tumor-associated vessels; in addition, primary B-Raf-deficient endothelial cells did not show any defects in sprouting, migration and proliferation in *in vitro* assays [58].

In this work, we investigated the phenotype of B-Raf Tie2Cre mice in detail to unravel the mechanism underlying accelerated LLC-1 tumor growth. We wanted to know

which properties of blood vessels are altered in the B-Raf Tie2Cre mice and how these changes lead to accelerated allograft growth. To address this question we investigated the functionality of vessels, measured by the extent of perfusion, the pericyte coverage and the vessel permeability. In addition, we wanted to investigate whether the function of B-Raf was endothelial cell-autonomous, or whether myeloid cells, also B-Raf-deficient in our model system, contributed to the phenotype.

3. Results

3.1. B-Raf Tie2Cre mice show accelerated tumor growth

To verify the phenotype of B-Raf Tie2Cre mice we repeated the injection of Lewis lung carcinoma (LLC-1) cells to study allograft tumor growth. The tumor cells were injected subcutaneously into the flank of B-Raf F/F Tie2Cre mice and B-Raf F/F mice as a control. As already shown, the mice with endothelial cell specific B-Raf deletion (B-Raf EC KO) showed accelerated tumor growth compared to the control mice (Fig.6.a).

Further analysis of the data revealed a large difference in the growth of tumors implanted in male versus female host, irrespective of the host genotype. Tumors from male B-Raf EC KO mice showed significant larger tumor volume and weight compared to control. Tumors implanted in females generally reached only about half the size of those implanted in males. Tumor growth was accelerated in B-Raf EC KO compared to wild-type females, but the difference was not significant (Fig.6.b,c). Therefore, only male animals were used for further analyses and experiments.

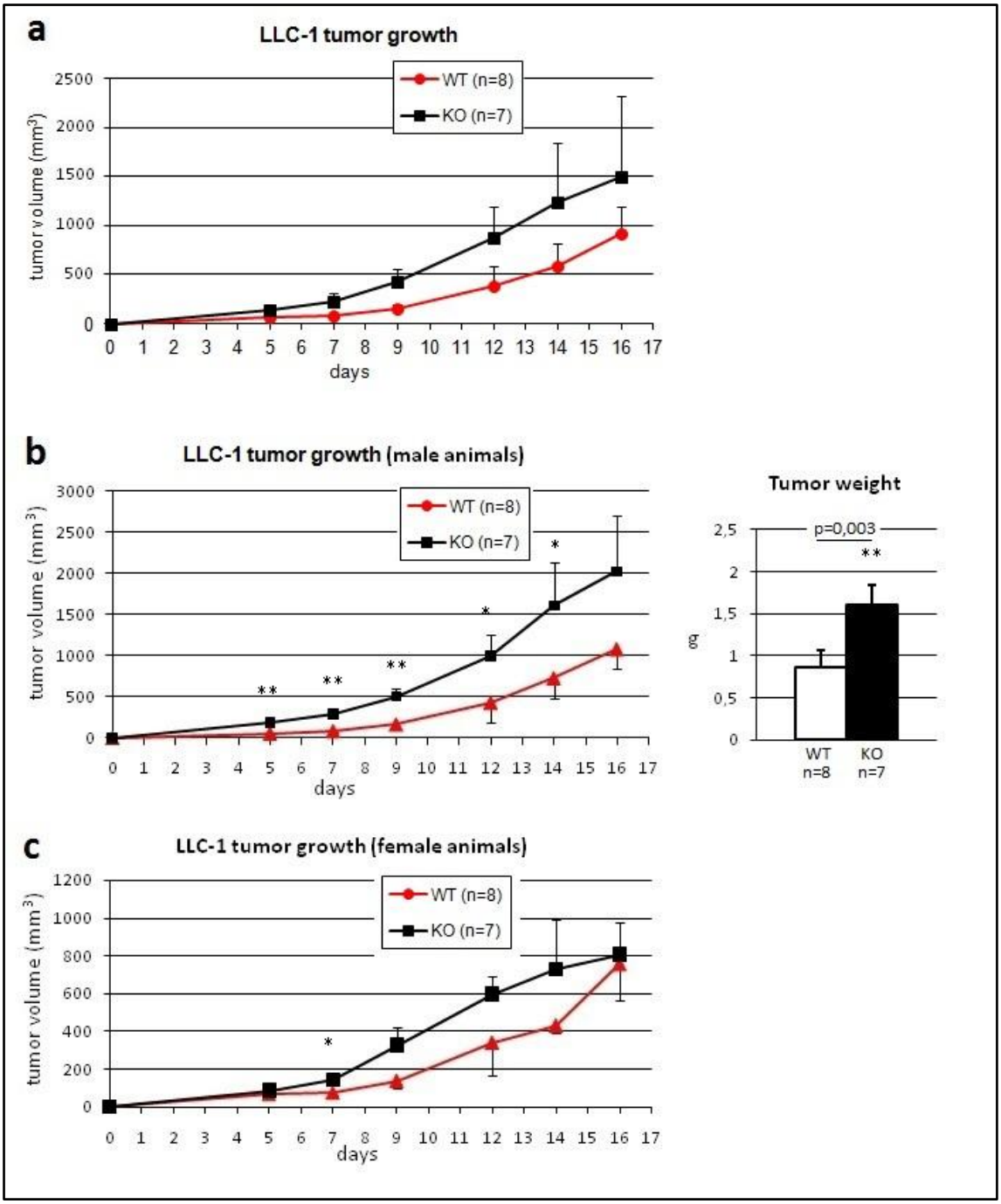

Fig.6. Growth curves of subcutaneous LLC-1 allograft tumors in B-Raf Tie2Cre and control mice. Tumor volume was calculated by measuring length and width of the tumor with a caliper. a. Tumor growth curve in male and female animals, compared with growth in male animals (b; right panel shows the tumor weight at day 16 post-implantation) or growth in female animals (c).

3.2. B-Raf EC KO tumors have the same quantity of vessels as control tumors

Tumors isolated from B-Raf EC KO or wild-type mice were either embedded in paraffin or frozen in a medium that provides a matrix ideal for cutting frozen sections for further analysis. Our main interest was the endothelial compartment, because at this point it was very likely that the tumors from B-Raf EC KO mice grew faster because of better vascularization. The number of vessels was similar in tumors isolated from B-Raf EC KO or wild-type animals. Vessel density was quantified by counting single vessels, visualized by the endothelial cell specific marker CD31 [59], in 2µm thick sections. To verify this, we additionally monitored the area of $CD31^+$ vessels, to be sure that there is no difference in the extent of vascularization. To achieve this, we prepared 40 – 50µm thick cryosections which allow visualization of vessel structure in a defined 3 dimensional area. The cryosections were stained with an CD31 antibody and whole z-stack of images were acquired using a confocal microscope. The z-stacks can be projected along the y-axis into one picture, reconstructing the structure of a vessel in a certain area with up to 40µm thickness. Quantification of the area of $CD31^+$ vessels in tumor sections with ImageJ showed no difference in vessel-occupied area within the tumors of B-Raf EC KO mice and control (Fig.7.a-b). Also the distribution between large and small vessels, judged by their area, did not vary between B-Raf EC KO and control (Fig.7.c).

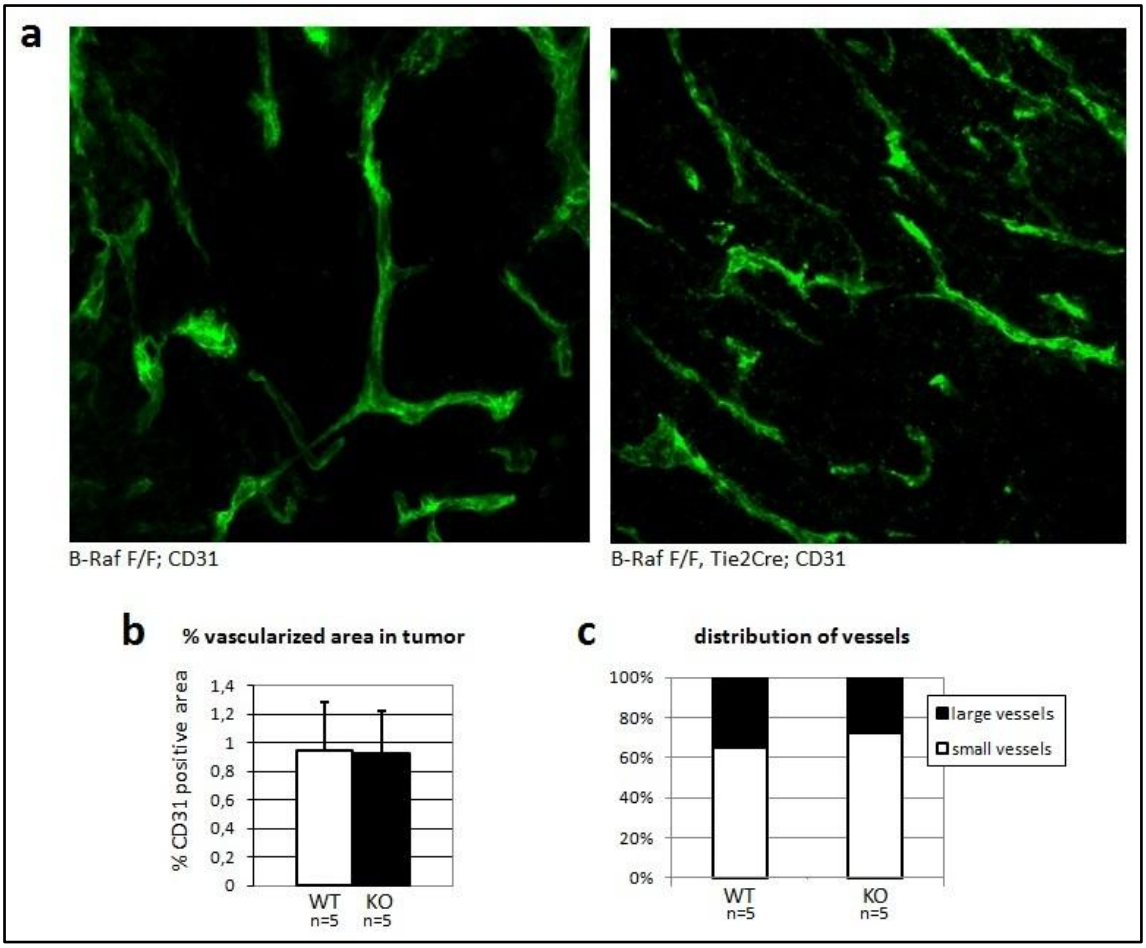

Fig.7. CD31 positive vessels. a. Projected photo stack of B-Raf EC KO tumor section (right) and control (left) labeled with a CD31 antibody. b. Quantification of CD31 positive area per picture. c. Quantification of the distribution of vessels in large (ImageJ: vessel area in picture >6%) and small (ImageJ: vessel area in picture <6%).

3.3. B-Raf EC KO tumors have the same number of perfused vessels as control

The tumors of B-Raf EC KO tumors are larger than control and show less necrosis. This led to the assumption that they might be better supplied with nutrients and oxygen. Since the number of blood vessels was the same, maybe the quality of the B-Raf EC KO tumor vessels was improved. This would mean a normalized vasculature, optimally providing the tumor with oxygen. We wanted to investigate if the number of perfused vessels, i.e. of the vessels actively connected to the blood circulation of the animal,

was increased in B-Raf EC KO tumors. Therefore we injected a fluorescence-labeled lectin, which binds specifically to endothelial cells, in the orbital plexus of tumor bearing mice. This technique visualizes only functional, actively perfused vessels, in contrast to the CD31 staining, which labels all endothelial cells. Using this staining, we could conclude that the total quantity of perfused vessels in tumor growing in B-Raf KO EC and wild-type animals was similar. Vessel density in highly perfused areas mainly located at the border of the tumor, an indicator for invasion of blood vessels into the tumor and/or more indirect for the extent of branching and network formation, was also similar in control and B-Raf KO EC mice (Fig.8.).

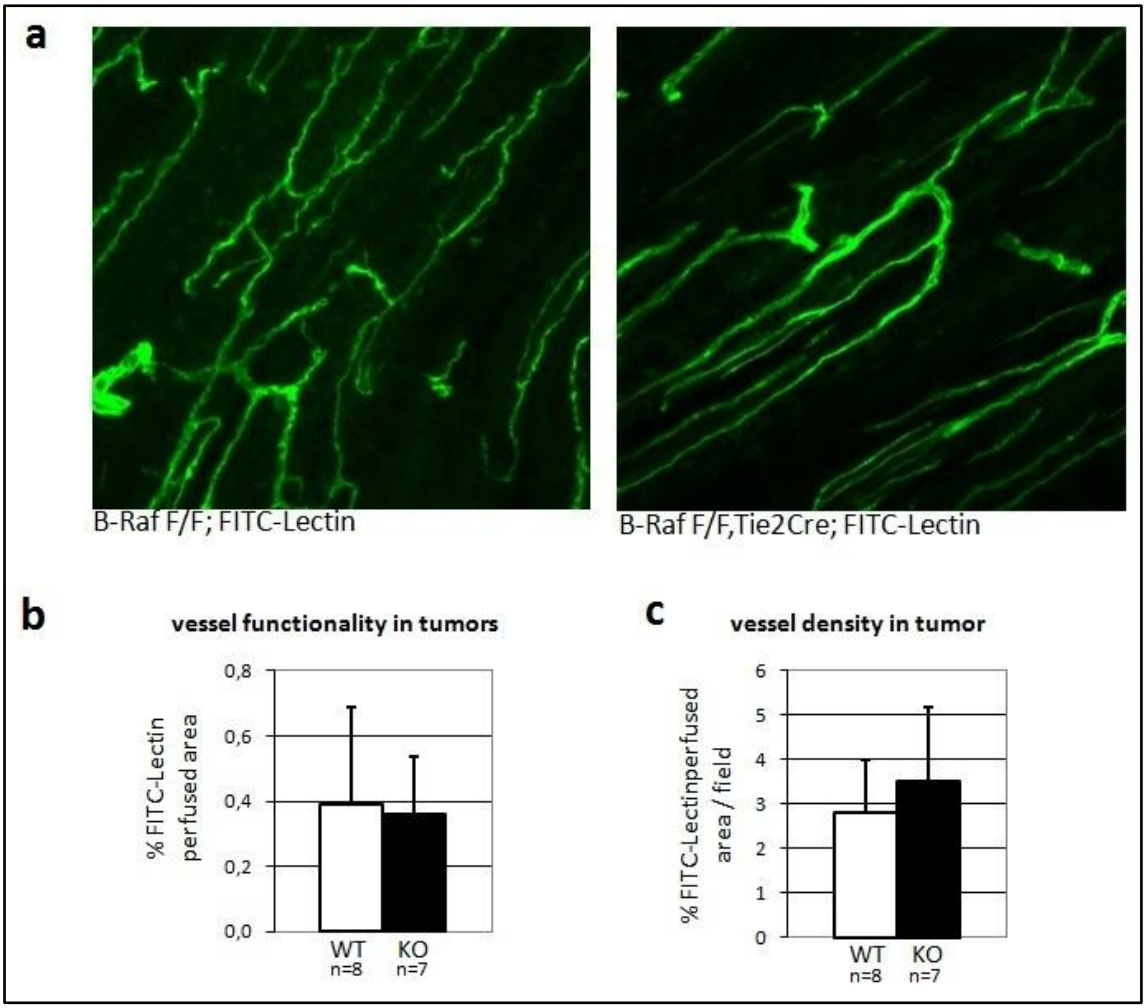

Fig.8. Vessel functionality. a. Projected image stack of tumors implanted in B-Raf EC KO (right) or control (left) mice. The vessels were labeled with FITC-Lectin. b. Quantification of the FITC-Lectin positive area in the whole section. c. Quantification of vessel density.

3.4. B-Raf EC KO tumors have the same extent of pericyte coverage as control

Next, we wanted to assess the pericyte coverage of tumor blood vessels. It is possible, that vessels in the B-Raf EC KO tumors are normalized in comparison to control because of more pericytes associated with endothelial cells. Pericytes stabilize the vasculature and are important for the regulation of vessel functionality, steady blood flow and quiescence of endothelial cells. We performed a double staining on frozen sections with CD31 and NG2, a marker specific for pericytes. The area of pericytes in close proximity to $CD31^+$ blood vessels, was calculated and expressed as % pericyte coverage. We found no difference in the number of pericytes associated with vessels in tumors growing in B-Raf EC KO and control mice (Fig.9.a-b).

A more detailed analysis, performed by grouping the vessels according to their size, showed that vessels were covered with a higher number of pericytes, but failed to reveal any difference between B-Raf EC KO and control vessels (Fig.9.c).

The vessels were further categorized in 3 classes, according to their extent of pericyte coverage (less than 5% coverage, between 5 and 15% coverage and more than 15% coverage) to monitor the contribution of vessels to each subclass in KO and WT. In B-Raf EC KO, as well as in control mice, the class of vessels with 5 – 15% pericyte coverage was the largest, followed by less than 5% coverage and more than 15% coverage (Fig.9.d). The pericyte coverage of B-Raf EC KO tumor-associated vessels can therefore be considered as unchanged compared to control.

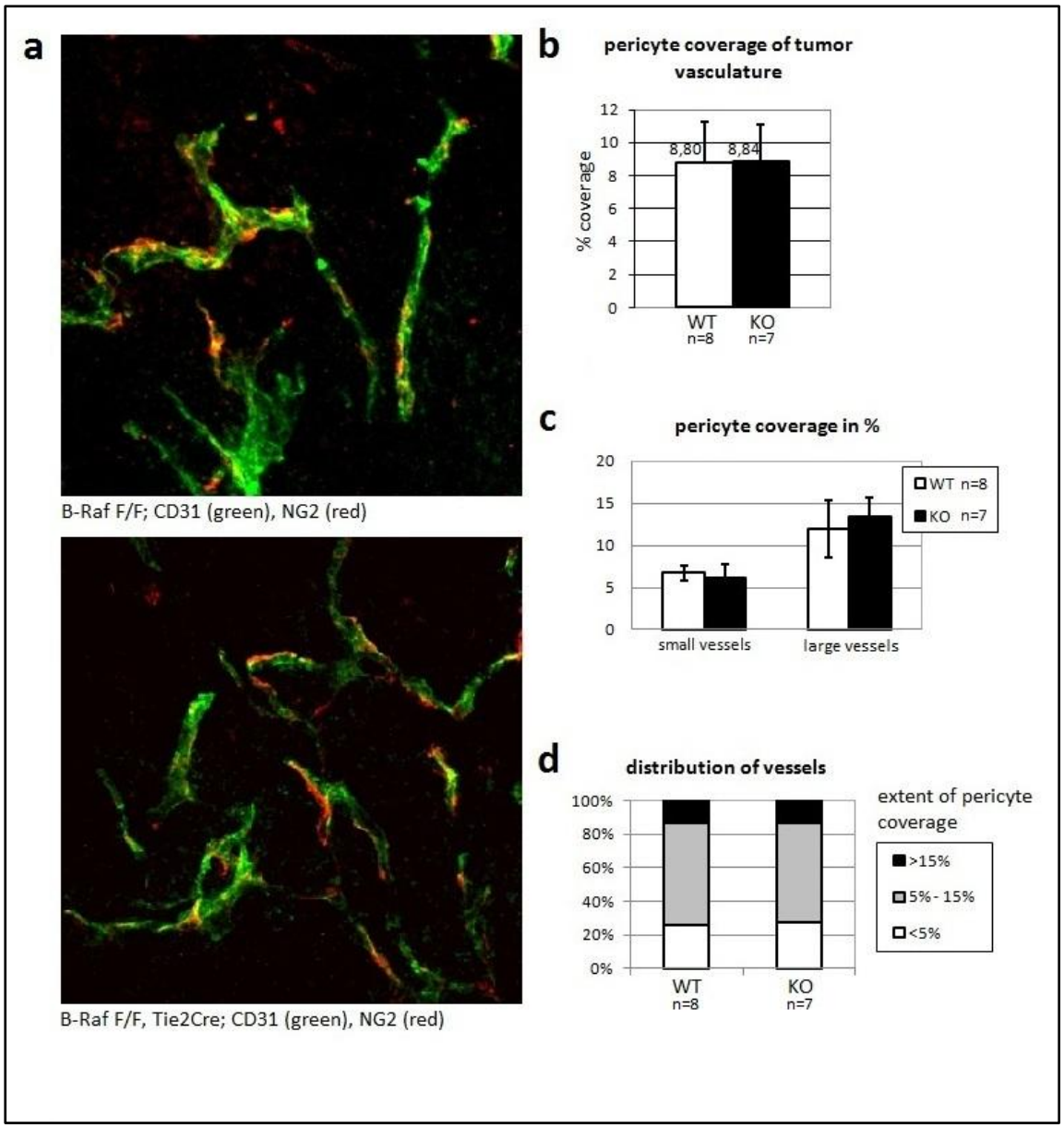

Fig.9. Pericyte coverage of tumor blood vessels. a. Projected stack of tumor sections isolated from B-Raf EC KO (lower picture) and control mice (upper picture) labeled with CD31 and NG2 antibodies to stain endothelial cells and pericytes, respectively. b. Quantification of the area of EC associated pericytes. c. Quantification of the area of EC associated pericytes specified for small and large vessels. The size of vessels is given in pixel. A vessel with an area below 1000pix^2 is considered as a small vessel, in contrast to a large vessel with more than 1000pix^2. One pixel is 1,85x10^{-4} mm. d. Quantification of the distribution of blood vessels according to their degree of pericyte coverage.

3.5. B-Raf EC KO mice show reduced VEGF stimulated permeability

Taking together the similar numbers of perfused vessel and the similar pericyte coverage, vessel functionality didn't seem enhanced in B-Raf EC KO mice so far. As the next parameter, we analyzed the permeability of blood vessels, since it is known that tumor-associated vessels in general show abnormally high permeability. We performed a Miles Assay that measures vessel permeability as a response to a stimulus such as VEGF. First, we injected Evans blue dye retroorbitally into mice. The dye enters the circulation and remains in the blood vessels, except at sites with decreased barrier function. We then stimulated permeability by intradermal injection of VEGF or PBS as a control. The dye leaking out of the vessel at the injection site is a measure of the permeability induced by the stimulus. We quantified leakage of Evans blue by measuring absorption with a spectral photometer after excising the skin and extracting the dye.

The total value of Evans blue extracted from the PBS injection site, reflecting the permeability of vessels without any angiogenic stimulus, was not significantly different in B-Raf EC KO mice and control mice (Fig10.a). VEGF induced permeability was calculated by subtracting the PBS-induced leakage from the amount of Evans blue leaked from the VEGF injection site, to minimize the influence of differences in general permeability, which were quite high between individuals. In control mice, the VEGF injection stimulated permeability 2.5-fold. The B-Raf EC KO mice in contrast showed only about 1.4-fold induction (Fig10.b-c). This result was barely significant ($p = 0,0511$), and showed a strong trend that led to further investigation of vessel permeability in the B-Raf EC KO animals.

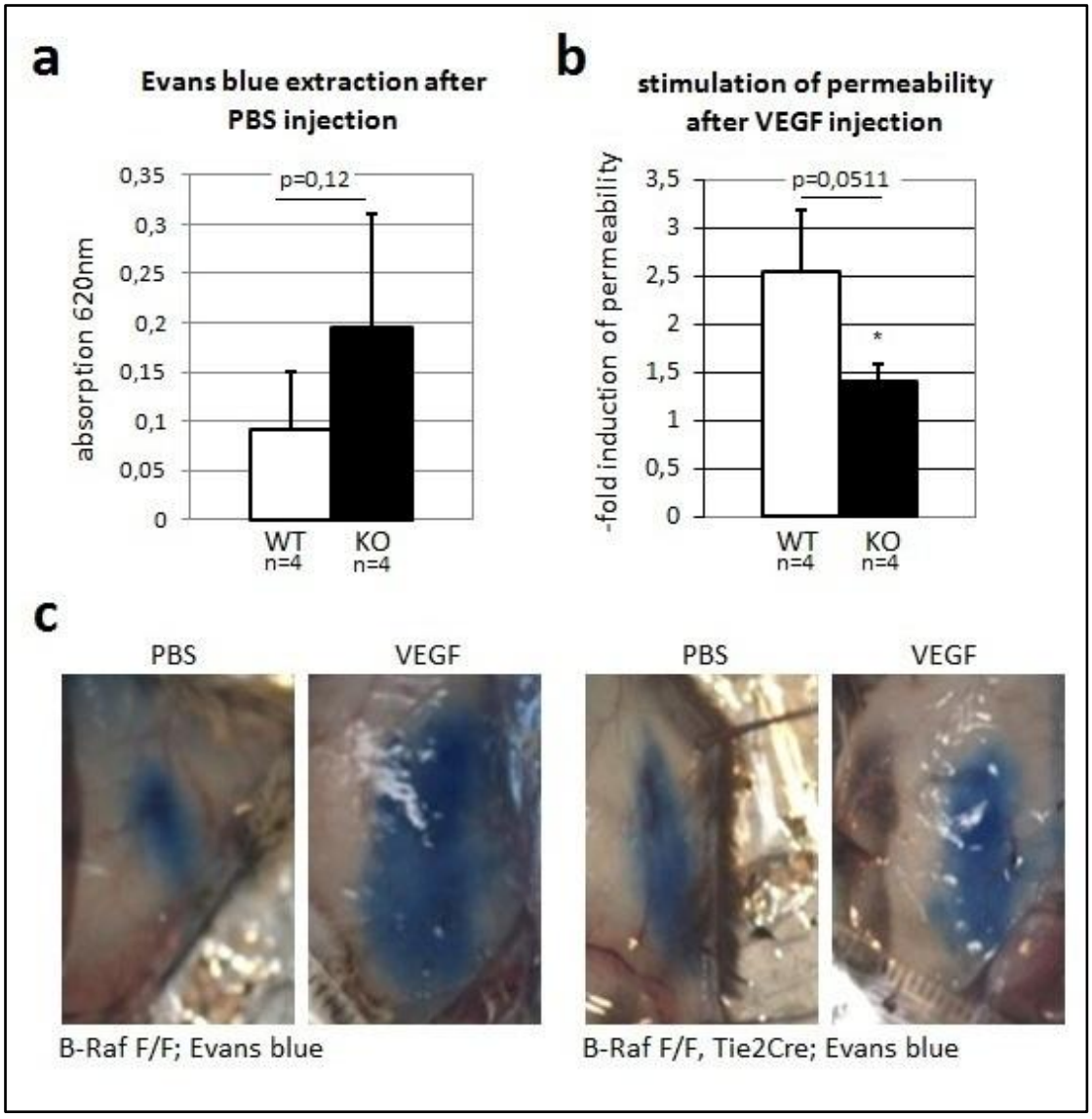

Fig.10. Miles Assay. a. Total PBS induced permeability. b. Relative VEGF induced permeability. c. Evans blue dye leaking out of skin from B-Raf EC KO animals (right) and control animals (left) after intradermal injection of PBS and VEGF, respectively.

3.6. B-Raf EC KO mice show reduced permeability in tumors

To further investigate whether reduced permeability, and therefore vessel normalization, could be the reason for the accelerated tumor growth in B-Raf Tie2Cre mice, we assessed permeability directly in tumor tissue by injecting Evans blue dye in tumor bearing B-Raf EC KO and control mice and calculating the amount of dye leaking

out relative to the weight of the tumor. As a control, we quantified vessel permeability in liver and lung. We found significantly reduced blood vessel permeability in the tumors developing in B-Raf EC KO animals compared to control, whereas in the control organs there was no difference (Fig.11.). This result indicates that the vessels of the B-Raf EC KO animals are less permeable specifically in the tumor, where we have an environment with abnormally high concentrations of pro-angiogenic factors. Less permeable vessels could be beneficial for tumor growth, because normalization of the tumor vasculature could help deliver nutrients and oxygen more efficiently especially to inner parts of the tumor.

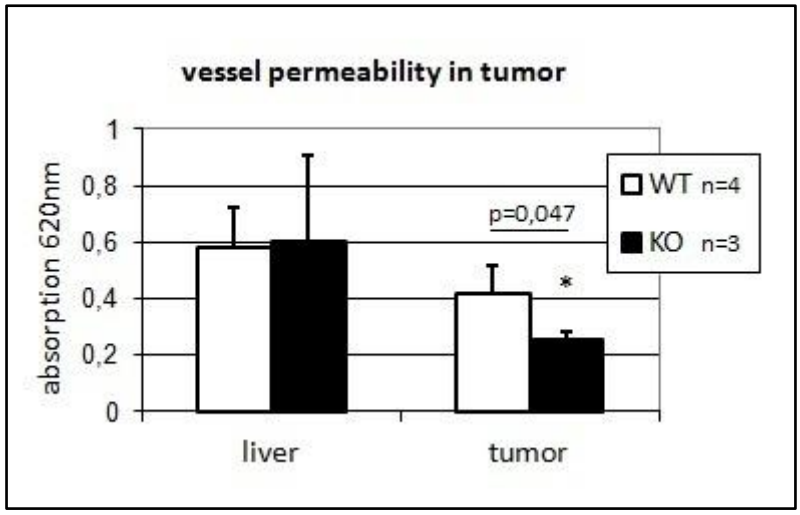

Fig.11. Quantification of Evans blue extraction from liver and tumor from B-Raf EC KO animals and control animals.

3.7. B-Raf KO ECs show reduced VEGF stimulated permeability in vitro

To verify the in vivo results from the experiments with Evans blue dye, we analyzed permeability of endothelial cells in vitro. We isolated primary mouse lung endothelial cells from B-Raf EC KO mice and control. For the permeability assessment we used a real-time cell analyzer that measures the impedance of a monolayer of cells. The impedance changes according to the electrical resistance generated by the monolayer,

which in turn is dependent on cell-cell contacts. Loosening or strengthening of cell-cell contacts in a monolayer of endothelial cells resembles what we call permeability in vivo, therefore the impedance measurement provides direct information about permeability under the right conditions. For this assay we used primary endothelial cells as well as immortalized ECs.

Monolayer formation was monitored by eye using a microscope. Permeability-enhancing stimuli were added to the cells while impedance measurement was performed every 15 seconds. As a result, we could show the reaction of the cells to the stimuli as well as the recovery in real-time.

The unstimulated monolayer of B-Raf KO and control cells did not show any difference in general barrier function. After stimulation with VEGF endothelial cells normally loosen their cell-cell contacts and therefore permeability is enhanced. This effect was clearly evident in real-time cell analyzer. In the curve (Fig.12.e) the Cell Index, which is a unit-less quantity the software calculates from the impedance, decreases after stimulation with VEGF. This means that the monolayer becomes more permeable. The primary B-Raf KO ECs, and even more prominently the immortalized ECs show a significant disability to react to VEGF with increased permeability (Fig.12.a and b+e). B-Raf KO ECs do not show any problems to react to other stimuli such as Thrombin that also enhances permeability of endothelial cells by elevating intracellular Ca^{2+} levels achieved by the activation of various signaling pathways that are partially the same and partially different than the pathways activated by VEGF signaling [60] (Fig.12.c-d). This indicates a selective defect of B-Raf KO ECs in reacting to VEGF, whereas other stimuli elicit a normal response.

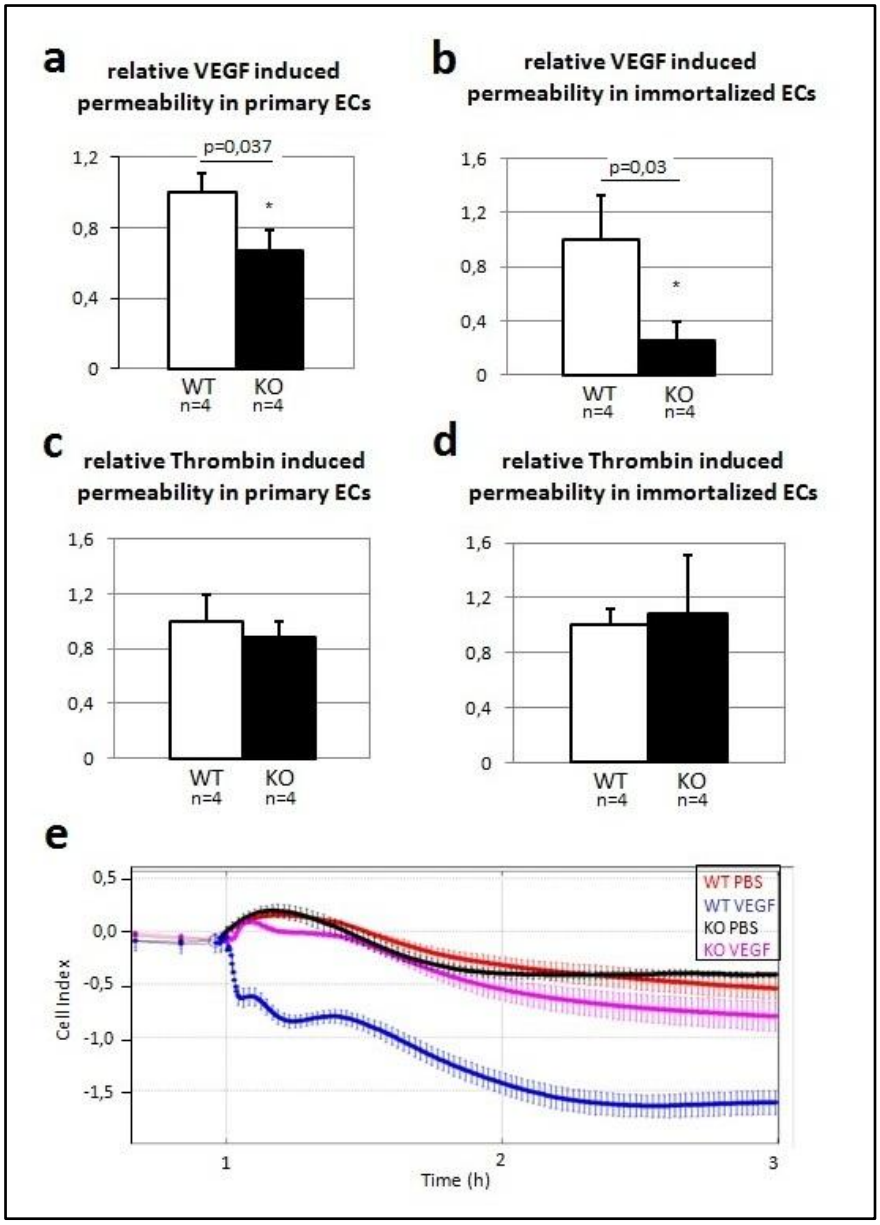

Fig.12. In vitro permeability assay. a-d. Permeability of isolated primary endothelial cells (a+c) and immortalized endothelial cells (b+d) treated with different stimuli. e. Example of a graph showing impedance measurement by the real-time cell analyzer. A monolayer of immortalized cells was treated with VEGF or PBS respectively, impedance was measured every 15 seconds after 1h of stimulation. Cell Index is a unit-less quantity calculated directly from the impedance and provides direct information about the permeability of the monolayer.

3.8. B-Raf knock-out in myeloid cells does not affect LLC-1 tumor growth

Tie2Cre recombinase deletes not only in endothelial cells, but also in hematopoietic cells. Therefore, B-Raf deletion also occurs in myeloid cells (macrophages, dendritic cells and granulocytes), T- and B-Lymphocytes, and NK cells [61], all of which can have a strong impact on tumor growth. Macrophages especially can influence tumor growth positively or negatively [41-42, 62], and have an impact on tumor angiogenesis [44, 46]. Therefore it is very important for us to investigate whether macrophages play a role in our system and if so, how much they contribute to the phenotype of accelerated tumor growth in B-Raf Tie2Cre mice.

To investigate the impact of the deletion of B-Raf in macrophages, we crossed a LysMCre transgenic line, expressing a Cre recombinase active only in the myeloid compartment [63], with B-Raf F/F mice and obtained offspring (B-Raf myeloid cell (MC) KO) with a myeloid-specific knock-out of B-Raf, as demonstrated by PCR of peritoneal macrophages. LLC-1 tumor allografts injected in these mice were indistinguishable in volume and weight from those implanted in wild-type animals (Fig.13), indicating that myeloid B-Raf does not have a crucial function in LLC-1 tumor growth in our system. We had no opportunity to investigate lymphocytes and NK cells, therefore the impact of B-Raf in those cells is unknown. In addition we made no distinction between lymphatic endothelial cells and blood vessel endothelial cells. Taken together, the results obtained in vivo with the B-Raf EC and B-Raf MC KO and the results obtained in vitro with B-Raf deficient endothelial cells are consistent with the hypothesis that accelerated tumor growth results from the knock-out of B-Raf in endothelial cells, leading to vessel normalization.

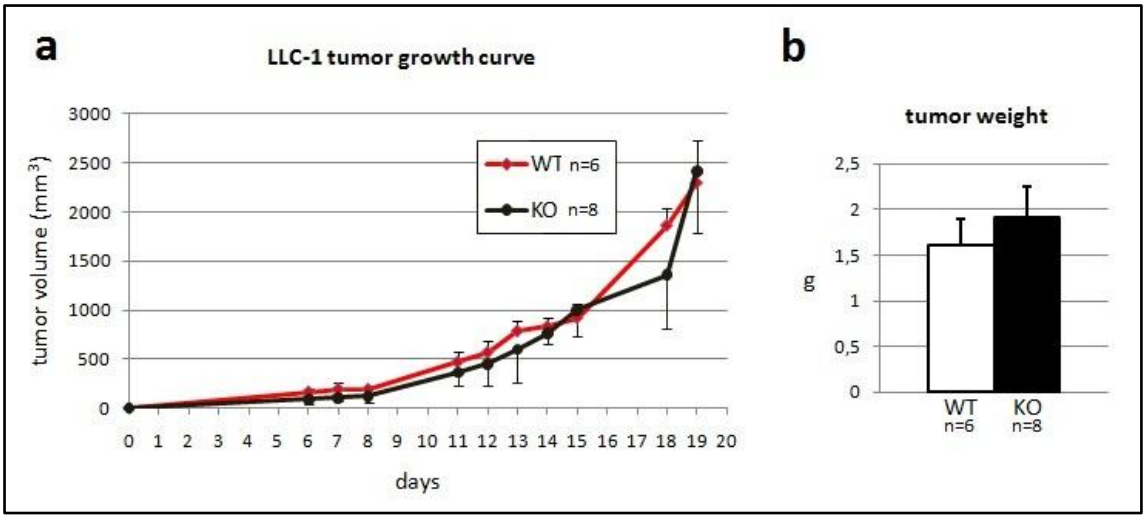

Fig.13. a. Growth of subcutaneous LLC-1 allograft tumors in B-Raf LysMCre and control mice. Tumor volume was calculated after measuring length and width of the tumor with a caliper. b. Tumor weight at day 19 after dissection of tumors.

4. Discussion

This work focused on the function of B-Raf in tumor-associated endothelial cells. Conventional deletion of B-Raf results in embryonic lethality due to reduced VEGF production and vascularization in the placenta[53]. To investigate whether B-Raf has an essential function in endothelial cells we worked with a conditional knock-out, the B-Raf EC KO mice. These mice lack apparent phenotypes unless challenged with allograft LLC-1 tumors, which grow faster in B-Raf EC KO animals of injected cells. The allografts are larger than those grown in control mice, and contain less necrotic area despite having the same number of blood vessels. We therefore hypothesized that the B-Raf EC KO tumors are better supplied with nutrients and oxygen, which, in turn, could be explained with enhanced functionality of the B-Raf EC KO vessels.

Neither active perfusion of tumor vessels by blood circulation nor pericyte coverage were altered in the B-Raf EC KO mice. However, skin blood vessels of the B-Raf EC KO mice were less capable of reacting to a VEGF injection by increasing permeability than vessels of the control mice. More importantly, the tumor vessels of B-Raf EC KO mice were less permeable than the control tumor vessels; consistent with these in vivo data, B-Raf-deficient endothelial cells were not able to react to VEGF stimulus with increased permeability to the same extent as control cells. These data indicate that the enhanced allograft growth observed in B-Raf EC KO mice is due to decreased EC permeability, which leads to vessel normalization.

Tie2Cre is active in both endothelial cells and bone marrow, and macrophages have been proposed to play an important role in vessel stability, by secreting VEGF [64]. The Baccarini lab has previously shown that B-Raf and ERK are necessary for VEGF production in a model of insulinoma [65]. We therefore investigated the involvement of macrophages in the growth of LLC-1 allografts in a mouse line lacking B-Raf in myeloid cells; tumors developed normally in these mice indicating that B-Raf ablation in myeloid cells does not contribute to the phenotype observed in the B-Raf EC KO system.

We observed a significant difference in LLC-1 allograft growth between sexes irrespective of the host genotype. There are many reports on the impact of sex hormones on tumor growth, but those studies usually concentrate on hormone-dependent cancers affecting breast, endometrium, ovary and prostate [66]. In non-sex hormone-dependent cancers the impact of sex is not determined. For adeno-carcinomas it is reported that estrogen has a tumor promoting role in a mouse model [67]. In humans, estrogen can be a risk factor for cancer development or have a protecting effect against cancers such as hepatocellular carcinoma [68]. The latter effect is based on the anti-inflammatory effects of estrogens, namely the down-regulation of IL-6 in macrophages [69]. Other studies have shown that females are less susceptible to cancer development in tissues that are not conventional targets of sex hormones [70].

However, for LLC-1 allografts in mice there is no reported influence of sex on tumor growth. So we can only speculate that female animals are protected against inflammation by estrogens in our model and therefore tumor growth is delayed.

Taken together, our findings indicate that under pathological conditions endothelial cell B-Raf contributes to a state of hyperpermeability of tumor-associated blood vessels caused by VEGF (Fig.14). According to this theory, B-Raf EC KO mice show an accelerated tumor growth because the tumor blood vessels are less leaky and therefore abler to provide the tumor with nutrients and oxygen [64, 71].

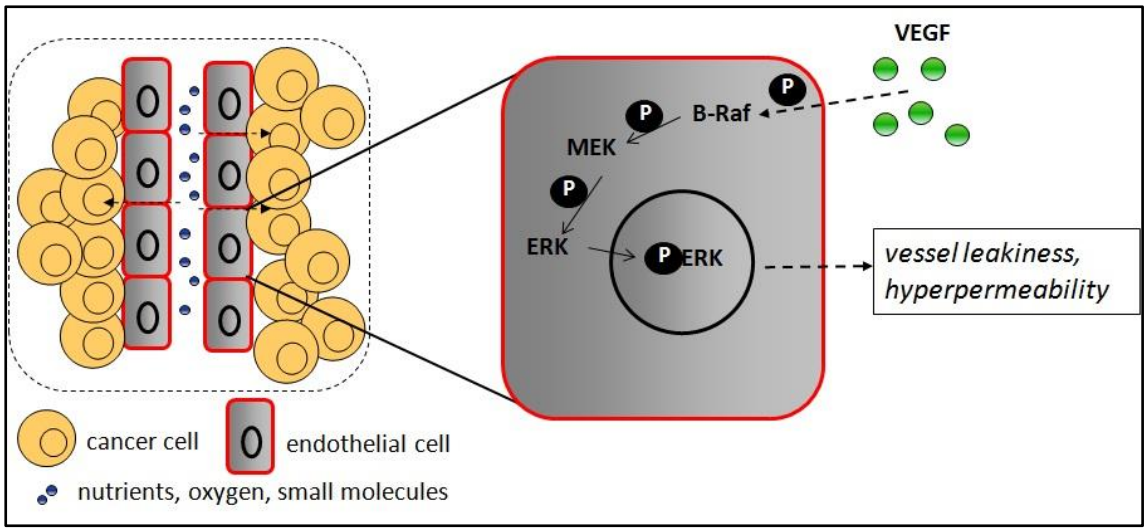

Fig.14. Current working model.

Mechanistically, we can only speculate how the regulation of permeability via B-Raf occurs. Most likely Erk is the key player downstream of B-Raf, since Erk is known to be upregulated downstream of VEGF signaling [72].

Several studies have shown that downregulation of Erk in endothelial cells can lead to decreased permeability. Breslin et al. has published that VEGF increases permeability in HUVECs and that this increase is attenuated by pretreatment with a MEK inhibitor and abolished by depletion of Erk. [73]. Similar experiments with bovine lung microvascular endothelial cells (BLMVECs) support the theory of MEK and Erk playing a role in hyperpermeability caused by 4-HNE, a product generated in the cell after oxidative stress [74]. In vivo, it has been demonstrated that exposure of mice to aerosols containing the bacterial endotoxin LPS enhances permeability of pulmonary vessels in an indirect manner by stimulating different cell types in the lung to produce permeability enhancing factors, such as cytokines and VEGF. Increased permeability correlates with Erk activation in the lung and can be reduced by co-administration of a MEK inhibitor. The fact that phosphorylated Erk was found at cell-cell borders after VEGF treatment strengthens the hypothesis that VEGF-mediated permeability enhancement is caused by Erk dependent myosin2 activation, leading to actin cytoskeleton rearrangements and to the disruption of cell-cell contacts [75].

These studies all highlight the importance of Erk and MAP kinase signaling in hyperpermeability induced by different stimuli. Assuming that in endothelial cells, as in other cells [53, 65, 76], B-Raf is the essential activator of MEK, a similar mechanism could underlie the decreased permeability of B-Raf-deficient vessels and monolayers.
Decreased intratumoral permeability may also lead to a partial normalization of the tumor-associated vasculature similar to the one achieved, at least in a small time window, by inhibiting VEGF [77], under which conditions blood flow, pericyte coverage or increased permeability were improved [21, 77]. Although we could not observe improvement of other blood vessel parameters such as increased perfusion or better pericyte coverage, in future it would be interesting to investigate whether tumors grown in B-Raf EC KO mice have also improved responsiveness to chemoradiation therapies. In fact, vessel normalization has been shown to increase tumor growth in some cases [64, 71], but decreases the metastatic potential of tumor cells [21]. Possible explanations for this phenomenon are reduction of interstitial pressure, acidosis and hypoxia in the tumor; and a block of tumor cell dissemination through improved endothelial barrier function. It would be interesting to examine if the endothelial deletion of B-Raf alters the metastatic behavior of LLC-1 cells in the mice.

The newly identified function of B-Raf in the tumor-associated vasculature could be of special relevance in tumor therapies where B-Raf inhibitors are already in use. Several studies with animal models as well as clinical studies in patients have shown that B-Raf inhibitors significantly increase therapeutic effect of other drugs, if they are administered as a combined treatment. Augustine et al. showed that the kinase inhibitor Sorafenib, that inhibits Raf amongst other kinases, significantly enhances the effect of chemotherapeutic drugs melphalan and temozolomide [78]. In a phase II clinical study sorafenib has been administered in combination with dacarbazine, which also led to a significantly increased therapeutic effect [79].
The underlying mechanism for the increased efficacy of chemotherapeutics administered in combination with Sorafenib is incompletely understood. Partially, the inhibition of MAP kinase signaling is responsible for the therapeutic benefits in

combined treatment [78]. Our results now show a normalization of tumor vasculature after deletion of B-Raf in endothelial cells. Although tumor growth is accelerated after the deletion of B-Raf in our mouse model, co-administration of chemotherapeutic drugs that target growth of cancer cells and inhibition of B-Raf in endothelial cells could lead to partial normalization of the tumor-associated vasculature, leading to better drug delivery and uptake in the tumor and ultimately to more effective tumor shrinkage.

5. Methods

Mice

All animal experiments were performed in accordance with a protocol authorized by the Austrian Ministry of Science and Communications, following the approval by the national Ethical Committee for Animal Experimentation.

Mice with endothelial and hematopoietic cell-restricted B-Raf deletion were obtained by crossing B-Raf flox/flox mice (F/F), in which B-Raf Exon 12 is flanked with LoxP sites, with mice expressing the Cre recombinase under the control of the Tie2 promoter[57]. Mice with myeloid cell-specific B-Raf deletion were obtained by crossing B-Raf F/F mice with mice expressing the Cre recombinase under the control of lysozyme M (LysM) promoter[63]. All experiments were performed using only mixed backround (129/Sv and C57BL/6; F1) male mice of 8 – 10 weeks of agewith.

EC isolation and culture

To obtain pure cultures of primary mouse endothelial cells (ECs) we isolated ECs from the lung, an organ ideal for EC isolation because of its high number of microvascular endothelial cells. The isolation was performed according to the protocol of Wimmer et al. (submitted manuscript). In brief, 5 – 13 days old mice were sacrificed, their lungs were excised, placed in cold EC Base Medium and quickly transferred to a cell culture dish. The lungs were minced with scissors and digested in 1 mg/ml Collagenase Type 1 (Worthington) for 1h at 37°C. Tissue clumps were crushed by passing the suspension through a 18G needle. To obtain single cells, the suspension was filtered through a cell strainer (70 µm mesh size; BD Falcon) prior to seeding on a cell culture dish pretreated with 2% gelatin (Sigma) and 10 µg/ml Fibronectin (Roche). The plates were washed with phosphate buffered saline (PBS) after 24 hours.

2 days after seeding the cells were incubated with dynabeads (Dynal Biotech) coated with anti-mouse ICAM-2 antibody (BD-Pharmingen) for 1h at 4°C. Cell-coated beads

were placed for 2 min in a Magnetic Particle Concentrator (Dynal), washed 4 times with EC Base Medium and seeded. The sorting procedure was repeated once after 2 more days.

Primary cells were cultured in EC Culture Medium and seeded on pretreated plates (2% gelatin (Sigma) and 10 µg/ml Fibronectin (Roche) over night at 37°C).

The immortalized cells were generated according to the protocol from Wimmer et al. (submitted manuscript) and cultured in EC Base Medium.

20x PBS: 180g NaCl, 6,4g NaH_2PO_4 and 21g Na_2HPO_4 were dissolved in 1l double-destilled Water (ddH_2O). pH was adjusted to 7,2 – 7,4 with HCl.

EC Base Medium: DMEM Medium supplemented with 1mM non-essential amino acids, 1mM sodium pyruvate (Gibco), 25 mM HEPES pH 7.4 (Applichem), 20% FBS (Sigma), 0,1g/l streptomycin and 0,06g/l penicillin.

EC Culture Medium: EC Base + 100 µg/ml Endothelial Mitogen (Biomedical Technologies Inc) and 100 µg/ml Heparin (Sigma).

Isolation of peritoneal Macrophages

To verify the deletion of B-Raf in macrophages of B-Raf LysMCre mice, we isolated macrophages from the peritoneal cavity of 7 weeks old mice injected intraperitoneally with 1ml Peptone (3% in H_2O), which leads to the accumulation of peritoneal macrophages. 5 days after injection, the mice were sacrificed . and their abdominal skin was carefully peeled back to expose the peritoneum. 10ml DMEM were injected carefully in the abdominal cavity and a peritoneal lavage was performed. The medium procedure was repeated once. The macrophages were pooled, centrifuged (300g, 5min) and cultured in Mϕ culture medium. After cultivation the medium of the cells needs to be replaced every 6 to 12 hours for 1 day.

Mϕ culture medium: DMEM medium supplemented with 10% FCS (Sigma), 10% Lcell conditoned medium (the filtered, cell-free supernatant of L929 mouse fibroblast cell line, which contains growth factors necessary for macrophage growth), 0,1 g/l streptomycin and 0,06g/l penicillin.

LLC-1 Allografts

For the tumor allograft experiments, injection of Lewis lung carcinoma cells (LLC-1), a well characterized laboratory mouse cancer cell line, was performed. LLC-1 cells were cultured in DMEM medium supplemented with 10% FBS (Sigma). No antibiotics were used to avoid indirect effects on the mouse after injection of the cells. To obtain subcutaneous tumor allografts in mice, 10^6 LLC-1 cells in 100µl PBS were injected subcutaneously into 8-10 weeks old male mice of mixed background (SV129/Bl6, F1) . The size of the arising tumors was measured every 2-3 days with a caliper, starting 7 days after injection of LLC-1 cells. Tumor volume was calculated according to the spheroid formula : $V=0,523*w^2*l$ (w= tumor with; l= tumor length). 16 days after implantation, the tumors were dissected and fast frozen in O.C.T. cryo compound (Tissue Tek), a premixed embedding medium ideal for frozen cutting, and stored at -20°C until further analysis.

FITC-Lectin injection

Functionality of tumor blood vessels was assessed by staining vessels connected to blood circulation of the animal with fluorescent labeled tomato lectin (FITC lectin) binding specifically to endothelial cells. FITC lectin (Vector Laboratories, 50µl of 2mg/ml solution) was injected retroorbitally into tumor-bearing mice 16 days after LLC-1 cell implantation. The mice were sacrificed 20min later and perfused with 20ml PBS followed by 20ml 4% paraformaldehyde (PFA) through the left heart ventricle.

Tumors and control tissue were fast frozen in O.C.T. cryo compound (Tissue Tek) on dry ice and stored at -20°C.

40-50µm thick sections were cut on a cryotome (MICROM HM 500 OM), placed on microscope slides (Thermoscientific Menzel-Glaeser Superfrost Plus) and air-dried for 20min in the dark. The tissue was fixed in 4% paraformaldehyde (PFA) for 1h, mounted (DAKO fluorescent mounting medium), sealed with a cover slip (Marienfeld Laboratory glassware) and dried overnight. The slides were inspected and imaged using a Confocal Microscope (Zeiss LSM Meta).

PFA solution 4%: 80g PFA with 2 – 4 NaOH pellets was dissolved in PBS at 56°C. The pH was adjusted to 7,2 with HCl and the final volume was 2l. Before use, the PFA solution needed to be filtered to get rid of insoluble remnants.

Miles Assay and Evans blue extraction from tumor

For analysis of permeability of skin blood vessels, the Miles Assay was performed according to previous described protocols [80]. In brief, Evans blue (1% in PBS, Sigma-Aldrich), a dye binding to plasma proteins and leaking out with them at sites of hyperpermeability, was injected retroorbitally in 12 weeks old male mice of mixed background (SV129/Bl6 F1) . 10min later, VEGF (R&D Systems, 50ng in 40-50µl PBS) or PBS were injected intradermally on either side of the flank. 20min later the mice were sacrificed and the skin of the injection sites was incubated in 2ml Formamide. The liver, used as a control organ, was incubated in 3ml Formamide. 4 days incubation at RT extracts the dye which can be measured directly by spectral photometry at 620nm wavelength.

Alternatively, tumor-bearing mice were injected retroorbitally with Evans blue 16 days after LLC-1 cells implantation. The mice were sacrificed 30min after injection and tumors and livers were isolated and placed in 3ml of Formamide. The extracted dye was calculated relative to tissue weight.

Immunofluorescence double staining for endothelial marker CD31 and pericyte marker NG2

We used frozen tumors for a double staining of endothelial cells (CD31 antibody) and pericytes (NG2 antibody) to monitor the pericyte coverage of blood vessels. 40-50µm thick sections were cut on a cryotome (MIRCROM HM 500 OM), dried 20min at RT and fixed with 4%PFA for 1h. Epitopes were retrieved by treatment with protease type XIV (Sigma cat nr.: P5147; 3,5U/ml for 8min,), followed by blocking of the endogenous peroxidase with 1.5% H_2O_2 for 40min. The slides were then blocked with blocking solution (normal goat serum NGS, Vector laboratories, cat nr.: s-1000, 0,5% in PBS) for 30min and incubated with rat anti-mouse CD31 (BD Pharmingen cat nr.: 550274; 1:50 in blocking solution) and rabbit anti-mouse NG2 (Millipore cat nr.: AB5320; 1:200 in blocking solution) overnight at 4°C. The slides were then incubated with the secondary antibody against CD31, horseradish peroxidase (HRP)-conjugated anti-rat (Amersham cat nr.: BA-4000, 1:1000 in blocking solution), for 1h at RT. The HRP signal was amplified using the Tyramide signal amplification TSA kit (PerkinElmer). The TSA reagent is a fluorophore-labelled tyramide, multiple copies of which are activated by the HRP moiety conjugated to the secondary antibody. The resulting short-lived tyramide radicals covalently bind to to residues in the vicinity of the HRP–target interaction site, leading to signal accumulation in the proximity of the antigen. . The slides were incubated with TSA green, a TSA reagent coupled to fluorescein, (1:100 in amplification diluent provided with the kit) for 10min at room temperature (RT) . The remaining HRP was inactivated using 5% H_2O_2 for 40min at RT. The secondary antibody against NG2, anti-rabbit HRP, was then applied for 1h at RT. In this case, the signal was amplified using TSA red, a TSA reagent coupled to tetramethylrhodamin, (1:100 in amplification diluent) for 10min at RT. DNA was stained with DAPI (1:3000 in PBS, 10min at RT) and the slides were mounted in a drop of fluorescent mounting medium (Dako) to reduce bleaching of the fluorophores and left to dry overnight. Between each of the steps, except after blocking, the slides were washed with TNT buffer (TSA

kit, PerkinElmer). The slides were inspected and imaged by confocal Microscopy using aZeiss LSM Meta.

20x TNT buffer (recipe from TSA kit, PerkinElmer): 242,28g Tris and 175,32g NaCl were dissolved in ddH_2O. The pH was adjusted to 7,5 with HCl and the final volume was 1l.

Real-time cell analysis

For real-time analysis of cell function we used the xCELLigence RTCA SP system (Roche) and the associated software (Roche). The real time cell analyzer (RTCA) measures electrical impedance (Z) across microelectrodes integrated into the bottom of special tissue culture plates (E-PLATES). Cells attaching to the plate on top of the electrodes lead to an increase in electrode impedance. The larger the area of the plate covered with cells, the stronger is the increase in impedance. The measurement is carried out over a defined time period and results in a curve that represents the biological status of the cells. Depending on the setup of the experiment, impedance measurement can give information about cell growth, morphology or adhesion. We used the RTCA to analyze barrier function of a monolayer of endothelial cells. An unstimulated, confluent monolayer of ECs generates stable electrical impedance. Addition of a permeability enhancing stimulus to the cells leads to loosening of cell-cell contacts resulting in a drop in electrical resistance that is measured in real-time by the RTCA.

10,000 immortalized ECs or 15,000 isolated primary ECs were seeded in one well of the E-PLATE VIEW 96 (Roche) respectively. For each condition, quadruplicates were performed. the RTCA measured impedance Overnight every 30min, yielding information on cell-substrate adhesion and cell-cell adhesion. After a period of about 12 hours the cells formed a monolayer yielding stable impedance measurements. Monolayer formation. was verified microscopically. Before addition of a stimulus the interval of impedance measurement was adjusted to 15 seconds, the shortest possible interval. VEGF (500ng/ml, R&D Systems cat nr.: V7259), Thrombin (10U/ml, Sigma-Aldrich cat nr.: T4648), or PBS as a control were added to all quadruplicate wells at

once using a multichannel pipette. The impedance measurement was continued for at least 3 hours after stimulus addition until the barrier function was clearly not decreasing any more.

Statistical Analysis

P values were calculated using the two-tailed Student's t test. A p value ≤ 0.05 is considered statistically significant. Each experiment was repeated at least 3 times. For experiments with mice, at least 4 animals per genotype and condition were used.

6. References

1. Jain, R.K., *Molecular regulation of vessel maturation.* Nat Med, 2003. **9**(6): p. 685-93.
2. Adams, R.H. and K. Alitalo, *Molecular regulation of angiogenesis and lymphangiogenesis.* Nat Rev Mol Cell Biol, 2007. **8**(6): p. 464-78.
3. Carmeliet, P., et al., *Abnormal blood vessel development and lethality in embryos lacking a single VEGF allele.* Nature, 1996. **380**(6573): p. 435-9.
4. Shalaby, F., et al., *Failure of blood-island formation and vasculogenesis in Flk-1-deficient mice.* Nature, 1995. **376**(6535): p. 62-6.
5. Shalaby, F., et al., *A requirement for Flk1 in primitive and definitive hematopoiesis and vasculogenesis.* Cell, 1997. **89**(6): p. 981-90.
6. Fong, G.H., et al., *Role of the Flt-1 receptor tyrosine kinase in regulating the assembly of vascular endothelium.* Nature, 1995. **376**(6535): p. 66-70.
7. Hellstrom, M., et al., *Lack of pericytes leads to endothelial hyperplasia and abnormal vascular morphogenesis.* J Cell Biol, 2001. **153**(3): p. 543-53.
8. Carmeliet, P., *Angiogenesis in life, disease and medicine.* Nature, 2005. **438**(7070): p. 932-6.
9. Nguyen, L.L. and P.A. D'Amore, *Cellular interactions in vascular growth and differentiation.* Int Rev Cytol, 2001. **204**: p. 1-48.
10. Olsson, A.K., et al., *VEGF receptor signalling - in control of vascular function.* Nat Rev Mol Cell Biol, 2006. **7**(5): p. 359-71.
11. Presta, M., et al., *Fibroblast growth factor/fibroblast growth factor receptor system in angiogenesis.* Cytokine Growth Factor Rev, 2005. **16**(2): p. 159-78.
12. Koblizek, T.I., et al., *Angiopoietin-1 induces sprouting angiogenesis in vitro.* Curr Biol, 1998. **8**(9): p. 529-32.
13. Bergers, G. and S. Song, *The role of pericytes in blood-vessel formation and maintenance.* Neuro Oncol, 2005. **7**(4): p. 452-64.
14. Sims, D.E., *Diversity within pericytes.* Clin Exp Pharmacol Physiol, 2000. **27**(10): p. 842-6.
15. Gaengel, K., et al., *Endothelial-mural cell signaling in vascular development and angiogenesis.* Arterioscler Thromb Vasc Biol, 2009. **29**(5): p. 630-8.
16. Folkman, J., *What is the evidence that tumors are angiogenesis dependent?* J Natl Cancer Inst, 1990. **82**(1): p. 4-6.
17. De Bock, K., et al., *Endothelial oxygen sensors regulate tumor vessel abnormalization by instructing phalanx endothelial cells.* J Mol Med, 2009. **87**(6): p. 561-9.
18. Greenberg, J.I., et al., *A role for VEGF as a negative regulator of pericyte function and vessel maturation.* Nature, 2008. **456**(7223): p. 809-13.
19. Maeda, H., *The enhanced permeability and retention (EPR) effect in tumor vasculature: the key role of tumor-selective macromolecular drug targeting.* Adv Enzyme Regul, 2001. **41**: p. 189-207.
20. McDonald, D.M. and P.L. Choyke, *Imaging of angiogenesis: from microscope to clinic.* Nat Med, 2003. **9**(6): p. 713-25.
21. Carmeliet, P. and R.K. Jain, *Principles and mechanisms of vessel normalization for cancer and other angiogenic diseases.* Nat Rev Drug Discov, 2011. **10**(6): p. 417-27.
22. De Bock, K., S. Cauwenberghs, and P. Carmeliet, *Vessel abnormalization: another hallmark of cancer? Molecular mechanisms and therapeutic implications.* Curr Opin Genet Dev, 2011. **21**(1): p. 73-9.

23. Jain, R.K., *Normalization of tumor vasculature: an emerging concept in antiangiogenic therapy.* Science, 2005. **307**(5706): p. 58-62.
24. Maeda, H., et al., *Vascular permeability enhancement in solid tumor: various factors, mechanisms involved and its implications.* Int Immunopharmacol, 2003. **3**(3): p. 319-28.
25. Folkman, J., *Tumor angiogenesis: therapeutic implications.* N Engl J Med, 1971. **285**(21): p. 1182-6.
26. Ellis, L.M. and D.J. Hicklin, *VEGF-targeted therapy: mechanisms of anti-tumour activity.* Nat Rev Cancer, 2008. **8**(8): p. 579-91.
27. Jain, R.K., *Antiangiogenic therapy for cancer: current and emerging concepts.* Oncology (Williston Park), 2005. **19**(4 Suppl 3): p. 7-16.
28. Bergers, G. and D. Hanahan, *Modes of resistance to anti-angiogenic therapy.* Nat Rev Cancer, 2008. **8**(8): p. 592-603.
29. Ghitescu, L., et al., *Specific binding sites for albumin restricted to plasmalemmal vesicles of continuous capillary endothelium: receptor-mediated transcytosis.* J Cell Biol, 1986. **102**(4): p. 1304-11.
30. Simionescu N. The Microvascular Endothelium: Segmental Differentiations`, Transcytosis`, Selective Distribution of Anionic Sites. New York: Raven`, 1979.
31. Dudek, S.M. and J.G. Garcia, *Cytoskeletal regulation of pulmonary vascular permeability.* J Appl Physiol, 2001. **91**(4): p. 1487-500.
32. Walter N. Durán`, Fabiola A. Sánchez`, Jerome W. Breslin. Microcirculatory Exchange Function. Compr Physiol 2011`, Supplement 9: Handbook of Physiology`, The Cardiovascular System`, Microcirculation: 81-124
33. Mehta, D. and A.B. Malik, *Signaling mechanisms regulating endothelial permeability.* Physiol Rev, 2006. **86**(1): p. 279-367.
34. Ferrara, N., *Vascular endothelial growth factor: molecular and biological aspects.* Curr Top Microbiol Immunol, 1999. **237**: p. 1-30.
35. Bates, D.O. and S.J. Harper, *Regulation of vascular permeability by vascular endothelial growth factors.* Vascul Pharmacol, 2002. **39**(4-5): p. 225-37.
36. Wu, H.M., et al., *Role of phospholipase C, protein kinase C, and calcium in VEGF-induced venular hyperpermeability.* Am J Physiol, 1999. **276**(2 Pt 2): p. H535-42.
37. Bates, D.O., et al., *Vascular endothelial growth factor increases Rana vascular permeability and compliance by different signalling pathways.* J Physiol, 2001. **533**(Pt 1): p. 263-72.
38. Vandenbroucke, E., et al., *Regulation of endothelial junctional permeability.* Ann N Y Acad Sci, 2008. **1123**: p. 134-45.
39. Goerdt, S. and C.E. Orfanos, *Other functions, other genes: alternative activation of antigen-presenting cells.* Immunity, 1999. **10**(2): p. 137-42.
40. Mantovani, G., et al., *Reactive oxygen species, antioxidant mechanisms and serum cytokine levels in cancer patients: impact of an antioxidant treatment.* J Cell Mol Med, 2002. **6**(4): p. 570-82.
41. Lewis, C.E. and J.W. Pollard, *Distinct role of macrophages in different tumor microenvironments.* Cancer Res, 2006. **66**(2): p. 605-12.
42. al-Sarireh, B. and O. Eremin, *Tumour-associated macrophages (TAMS): disordered function, immune suppression and progressive tumour growth.* J R Coll Surg Edinb, 2000. **45**(1): p. 1-16.
43. Hagemann, T., et al., *Macrophages induce invasiveness of epithelial cancer cells via NF-kappa B and JNK.* J Immunol, 2005. **175**(2): p. 1197-205.

44. De Palma, M., et al., *Tie2 identifies a hematopoietic lineage of proangiogenic monocytes required for tumor vessel formation and a mesenchymal population of pericyte progenitors.* Cancer Cell, 2005. **8**(3): p. 211-26.
45. Venneri, M.A., et al., *Identification of proangiogenic TIE2-expressing monocytes (TEMs) in human peripheral blood and cancer.* Blood, 2007. **109**(12): p. 5276-85.
46. Murdoch, C., et al., *The role of myeloid cells in the promotion of tumour angiogenesis.* Nat Rev Cancer, 2008. **8**(8): p. 618-31.
47. Baccarini, M., *Second nature: biological functions of the Raf-1 "kinase".* FEBS Lett, 2005. **579**(15): p. 3271-7.
48. Pritchard, C.A., et al., *Post-natal lethality and neurological and gastrointestinal defects in mice with targeted disruption of the A-Raf protein kinase gene.* Curr Biol, 1996. **6**(5): p. 614-7.
49. Huser, M., et al., *MEK kinase activity is not necessary for Raf-1 function.* EMBO J, 2001. **20**(8): p. 1940-51.
50. Mikula, M., et al., *Embryonic lethality and fetal liver apoptosis in mice lacking the c-raf-1 gene.* EMBO J, 2001. **20**(8): p. 1952-62.
51. Piazzolla, D., et al., *Raf-1 sets the threshold of Fas sensitivity by modulating Rok-alpha signaling.* J Cell Biol, 2005. **171**(6): p. 1013-22.
52. Wojnowski, L., et al., *Endothelial apoptosis in Braf-deficient mice.* Nat Genet, 1997. **16**(3): p. 293-7.
53. Galabova-Kovacs, G., et al., *Essential role of B-Raf in ERK activation during extraembryonic development.* Proc Natl Acad Sci U S A, 2006. **103**(5): p. 1325-30.
54. Vakiani, E. and D.B. Solit, *KRAS and BRAF: drug targets and predictive biomarkers.* J Pathol, 2011. **223**(2): p. 219-29.
55. Wan, P.T., et al., *Mechanism of activation of the RAF-ERK signaling pathway by oncogenic mutations of B-RAF.* Cell, 2004. **116**(6): p. 855-67.
56. Poulikakos, P.I., et al., *RAF inhibitors transactivate RAF dimers and ERK signalling in cells with wild-type BRAF.* Nature, 2010. **464**(7287): p. 427-30.
57. Kisanuki, Y.Y., et al., *Tie2-Cre transgenic mice: a new model for endothelial cell-lineage analysis in vivo.* Dev Biol, 2001. **230**(2): p. 230-42.
58. Scherrer`, K. Raf in Angiogenesis.Diploma thesis (2010).
59. Scherrer`, K. Raf in Angiogenesis. Diplomarbeit 2010
60. Kumar, P., et al., *Molecular mechanisms of endothelial hyperpermeability: implications in inflammation.* Expert Rev Mol Med, 2009. **11**: p. e19.
61. Constien, R., et al., *Characterization of a novel EGFP reporter mouse to monitor Cre recombination as demonstrated by a Tie2 Cre mouse line.* Genesis, 2001. **30**(1): p. 36-44.
62. Bingle, L., N.J. Brown, and C.E. Lewis, *The role of tumour-associated macrophages in tumour progression: implications for new anticancer therapies.* J Pathol, 2002. **196**(3): p. 254-65.
63. Clausen, B.E., et al., *Conditional gene targeting in macrophages and granulocytes using LysMcre mice.* Transgenic Res, 1999. **8**(4): p. 265-77.
64. Stockmann, C., et al., *Deletion of vascular endothelial growth factor in myeloid cells accelerates tumorigenesis.* Nature, 2008. **456**(7223): p. 814-8.
65. Sobczak, I., et al., *B-Raf is required for ERK activation and tumor progression in a mouse model of pancreatic beta-cell carcinogenesis.* Oncogene, 2008. **27**(35): p. 4779-87.
66. Key, T.J., et al., *Energy balance and cancer: the role of sex hormones.* Proc Nutr Soc, 2001. **60**(1): p. 81-9.

67. Hammoud, Z., et al., *Estrogen promotes tumor progression in a genetically defined mouse model of lung adenocarcinoma.* Endocr Relat Cancer, 2008. **15**(2): p. 475-83.
68. Stabile, L.P. and J.M. Siegfried, *Sex and gender differences in lung cancer.* J Gend Specif Med, 2003. **6**(1): p. 37-48.
69. Naugler, W.E., et al., *Gender disparity in liver cancer due to sex differences in MyD88-dependent IL-6 production.* Science, 2007. **317**(5834): p. 121-4.
70. Mantovani, A., et al., *Cancer-related inflammation.* Nature, 2008. **454**(7203): p. 436-44.
71. Hamzah, J., et al., *Vascular normalization in Rgs5-deficient tumours promotes immune destruction.* Nature, 2008. **453**(7193): p. 410-4.
72. Zachary, I., *VEGF signalling: integration and multi-tasking in endothelial cell biology.* Biochem Soc Trans, 2003. **31**(Pt 6): p. 1171-7.
73. Breslin, J.W., et al., *VEGF increases endothelial permeability by separate signaling pathways involving ERK-1/2 and nitric oxide.* Am J Physiol Heart Circ Physiol, 2003. **284**(1): p. H92-H100.
74. Usatyuk, P.V. and V. Natarajan, *Role of mitogen-activated protein kinases in 4-hydroxy-2-nonenal-induced actin remodeling and barrier function in endothelial cells.* J Biol Chem, 2004. **279**(12): p. 11789-97.
75. Stockton, R., et al., *Induction of vascular permeability: beta PIX and GIT1 scaffold the activation of extracellular signal-regulated kinase by PAK.* Mol Biol Cell, 2007. **18**(6): p. 2346-55.
76. Galabova-Kovacs, G., et al., *Essential role of B-Raf in oligodendrocyte maturation and myelination during postnatal central nervous system development.* J Cell Biol, 2008. **180**(5): p. 947-55.
77. Winkler, F., et al., *Kinetics of vascular normalization by VEGFR2 blockade governs brain tumor response to radiation: role of oxygenation, angiopoietin-1, and matrix metalloproteinases.* Cancer Cell, 2004. **6**(6): p. 553-63.
78. Augustine, C.K., et al., *Sorafenib, a multikinase inhibitor, enhances the response of melanoma to regional chemotherapy.* Mol Cancer Ther, 2010. **9**(7): p. 2090-101.
79. McDermott, D.F., et al., *Double-blind randomized phase II study of the combination of sorafenib and dacarbazine in patients with advanced melanoma: a report from the 11715 Study Group.* J Clin Oncol, 2008. **26**(13): p. 2178-85.
80. Fainaru, O., et al., *Doxycycline induces membrane expression of VE-cadherin on endothelial cells and prevents vascular hyperpermeability.* FASEB J, 2008. **22**(10): p. 3728-35.

7. Acknowledgements

In the first place I want to give thanks to Manuela for taking me into the lab, giving the project into my hands and for every encouraging word during discussions, seminars or just in a coffee break.

I want to thank the whole Baccarini lab, Florian, Bartek, Ines, Josipa, Botond, Eszti, Gabriele, Christian, Katka, Matthias, Anna, Veronika, Andrea, Clemens and Isabella for suggestions, tips and a lot of good advice not only for my project but in any means; for sharing reagents and techniques; for the cool lab trip; for super-funny lunch breaks; for happy hours in- and outside of MFPL; for the nice weddings; for the dirty gossiping; and finally for the good atmosphere in the lab. Needless to say the biggest thank-you is for Reiner for his endless patience.
Finally I thank everyone who contributed to this work in any way.

CV – Barbara Maier

Firstname: Barbara

Lastname: Maier

Contact information

Date of birth: 31.07.1987

Place of birth: Vienna, Austria

Nationality: Austria

Adress:

Street: Heigerleinstraße 55

City, postcode: 1170 Vienna

Country: Austria

Phone no. (home): 069911051072

Phone no. (work): 01427754629

e-mail: Barbara.Maier@univie.ac.at

Education

Primary school: 1993 – 1997 Lutherschule, 1180 Vienna

High school: 1997-2005, GRG Parhamerplatz, 1170 Vienna

University: University of Vienna

Date: 01.10.2005 – Summer 2011

Honours class: Master of Science (M.Sc)

Field of study: Molecular Biology

Internships:

Mar.-Apr. 2009: Lab. Technau, U. (Center for Organismal Systems Biology, University of Vienna)

Nov.-Dec. 2009: Lab. Jantsch, V. (MFPL)

Feb.-Mar. 2010: Lab. Martinez, J. (IMBA)

Diploma thesis:

June 2010 - June 2011: Lab. Baccarini, M. (MFPL)

"The Role of B-Raf in tumor-driven angiogenesis”